

DESIGN OF AN ULTRA LOW POWER CONTROL SYSTEM FOR A SELF-
POWERED WIRELESS SENSOR

By

DAVID EDWARD JOHNSON

A THESIS PRESENTED TO THE GRADUATE SCHOOL
OF THE UNIVERSITY OF FLORIDA IN PARTIAL FULFILLMENT
OF THE REQUIREMENTS FOR THE DEGREE OF
MASTER OF SCIENCE

UNIVERSITY OF FLORIDA

2006

Copyright 2006

by

David Edward Johnson

ACKNOWLEDGMENTS

I would like to thank my advisors, Toshikazu Nishida, Khai Ngo, Jenshan Lin, and Juan Nino, who provided encouragement and support in completing my thesis. My advisors also had an abundance of patience with me as I balanced a full time career with working on a master's degree, and for this I am deeply thankful. Specifically I would like to thank Toshikazu Nishida for giving me a job with IMG as an undergraduate, which provided me with the opportunity to work on remarkable research projects. The position with IMG definitely instilled a desire to continue my education. Many thanks go to my fellow students that worked on sections of the self-powered wireless sensor design. Specifically, thanks go to Jerry Jun and Ed Koush for their work and help with the RF transmitter characterization as well as their work with the hydrogen sensor. Thanks go to Shengwen Xu for his work on the energy reclamation circuit. Thanks go to Anurag Kasyap for his work on the piezoelectric beams. I would like to thank all of the members of IMG who allowed me to work freely in the lab and provided much needed assistance with the use of equipment. Thanks go to the staff at the University of Florida, including Linda Kahila, Shannon Chillingworth, and Janet Holman.

My employer, Cisco Systems, deserves special thanks for allowing me to continue my education while working full-time. I would like to explicitly thank my manager Phil Van Atta for his proctoring as well as his understanding and encouragement in completing my degree. I would also like to thank Frank Juliano for his assistance in covering my work at Cisco while I took trips to school in order to work on my thesis.

Special thanks go to a college roommate, Gregory Schaefer, who helped me in deciding to pursue an undergraduate degree in engineering, and ultimately a master's degree in engineering. I would like to thank Dr. Roland Federico and his family for allowing me the use of their condominium when I visited Gainesville to work on my thesis. I would like to thank my family and friends for their love and support. My deepest thanks go to Barbara Fleener, whose love and support have kept me motivated for the past few years. Finally, my thanks go to God for instilling the desire to learn within my soul.

TABLE OF CONTENTS

	<u>page</u>
ACKNOWLEDGMENTS	iii
LIST OF TABLES	vii
LIST OF FIGURES	viii
ABSTRACT	x
INTRODUCTION	1
Research Goals	3
Thesis Organization	4
THEORETICAL DEVELOPMENT	6
Background Information	6
Previous Work	7
Design Challenges	9
DESIGN OF A CONTROL SYSTEM FOR A SELF POWERED WIRELESS SENSOR	11
Selection of a Microcontroller	11
Design of Programming Code	14
Level Monitoring	15
Data Transmitting	16
Programming Techniques for Minimizing Power Consumption	18
RF Transmitter	21
Design of RF Transmitter	21
Power Consumption for a RF Transmitter	22
Free Space method	22
Plane Earth method	24
Techniques for minimizing power consumption	25
Construction of a Prototype	26
EXPERIMENTAL METHODS AND SETUP	31
Energy Sources	31

Energy from Light	31
Energy from Vibrations	32
Data Sensor	33
Testing Methodology for the Control System	36
Methods for Measuring Power Consumption.....	36
Methods for Characterizing RF Transmission	37
Testing of a Self-Powered Wireless Sensor.....	39
EXPERIMENTAL RESULTS.....	42
RF Transmitter Characterization	42
ADC Testing.....	44
Testing of the Control System	45
RF Transmission.....	45
Power Consumption	51
Functional Verification.....	64
System Integration.....	65
CONCLUSIONS.....	67
Conclusions.....	67
Future Work.....	68
MICROCONTROLLER PROGRAM CODE	70
Code for Level Monitoring.....	70
Code for Data Transmitting.....	72
LIST OF REFERENCES	75
BIOGRAPHICAL SKETCH	79

LIST OF TABLES

<u>Table</u>	<u>page</u>
3-1 Power characteristics of microcontrollers.	12
3-2 Added features of microcontrollers.	13
5-1 Maximum transmission distances for different antenna locations.	51

LIST OF FIGURES

<u>Figure</u>		<u>page</u>
2-1	Simple state machine of a control system for a wireless sensor.	10
3-1	System level block diagram of self powered wireless sensor.	11
3-2	Microcontroller flow chart for level monitoring.	15
3-3	Microcontroller flow chart for data transmitting.	17
3-4	Frequency versus current consumption for MSP430 operating at 3V.	19
3-5	Supply voltage versus current consumption for MSP430 operating at 32 kHz.	20
3-6	Schematic of TX-99 RF transmitter.	22
3-7	Transmission distance versus power loss for given frequencies.	23
3-8	Power loss vs. transmit distance for various transmitter and receiver heights.	25
3-9	Schematic for control system prototype.	27
3-10	Top side PCB layout for control system prototype.	28
3-11	Bottom side PCB layout for control system prototype.	29
3-12	Control system prototype with RF transmitter.	30
3-13	Top side of control system prototype.	30
4-1	Bimorph PZT composite beams.	33
4-2	Direct charging circuit for energy reclamation from vibrations.	33
4-3	Schematic of biasing circuit for hydrogen sensor.	35
4-4	Picture of biasing circuit with hydrogen sensor.	36
4-5	Whip antenna.	38
4-6	Floor layout of the atrium area in NEB.	38

4-7	Test setup.	39
4-8	Gas chamber for testing hydrogen sensor.	40
5-1	Transmit power from Ming TX-99 RF transmitter.	44
5-2	Received spectrum at 1 meter from transmitter.	46
5-3	Received spectrum at 8 meters from transmitter.	47
5-4	Received power at varying distance from transmitter.	48
5-5	Received signal at 8 meters.	49
5-6	Received signal at 10 meters.	50
5-7	Received signal at 14.5 meters.	51
5-8	Scope capture of voltage across series resistor during initialization.	53
5-9	Scope capture of voltage across series resistor during idle state.	54
5-10	Transmit power for a single data bit.	55
5-11	Zoomed in view of transmit power for a single data bit.	56
5-12	Scope capture of transmission power for data pattern '1011101011'.	58
5-13	Scope capture of transmission power for data pattern '1101100101'.	59
5-14	Scope capture of transmission power for data pattern '1010000110'.	60
5-15	Different data patterns for two "1" valued bits.	61
5-16	Maximum average transmission power vs. number of "1" valued bits.	62
5-17	Duty cycle vs. average power for level monitoring.	64

Abstract of Thesis Presented to the Graduate School
of the University of Florida in Partial Fulfillment of the
Requirements for the Degree of Master of Science

DESIGN OF AN ULTRA-LOW POWER CONTROL SYSTEM FOR A SELF-
POWERED WIRELESS SENSOR

By

David Edward Johnson

May 2006

Chair: Toshikazu Nishida

Major Department: Electrical and Computer Engineering

Wireless sensors are becoming more commonplace in applications where harsh environments or remote locations make it difficult to run wires. Making these sensors self-powered is essential as battery replacement is extremely difficult. The drawback of being self-powered is that the system must rely on the environment for power. With the small size of a wireless sensor in mind, the amount of energy available is minimal. Hence there is a need for a control system that manages when power is distributed to different portions of the design.

This thesis focuses on the design of a control system that manages the components of a self-powered wireless sensor, with optimization for ultra-low power. The control system was designed with several flexibilities, so it can be used to interface a variety of sensors. The control system consists of a Texas Instruments MSP430 microcontroller and a MING TX-99 RF transmitter. The MSP430 microcontroller has an analog to digital converter which is used to encode data from the sensor. One of the

output ports on the microcontroller is used to interface the TX-99 RF transmitter. One of the keys to minimizing power consumption is for the microcontroller to stay in a low power mode. The microcontroller supplies the data and power to the RF transmitter; so power can be minimized further by applying power to the transmitter only when data is being transmitted.

The power consumption of the control system is partitioned into three main portions: sensor sampling, data transmission, and idle time. The microcontroller code was written so that the average power used to sample data from a sensor was the same as the power to remain idle, which is $2.5\mu\text{W}$. The average power used to transmit a single bit is $261\mu\text{W}$. The code running on the microcontroller was written to be able to vary the idle time between sampling and transmissions. By allowing the idle time to be varied the total average power can be varied according to how often the end user wants to transmit data. Two modes of operation were designed, (1) threshold based and (2) data based, so that the design would have the flexibility of providing either level detection or data logging. The flexibility in the design while maintaining minimal power requirements allows this control system to work for a range of wireless sensor applications. The control system was tested with a ZnO nano-rod hydrogen sensor while being powered from both solar and piezoelectric energy.

CHAPTER 1 INTRODUCTION

Applications for wireless sensors are growing in many fields from environmental and health monitoring to disaster relief. Further applications for wireless sensors include space exploration, military uses, chemical processing and other fields where the environmental conditions make it extremely difficult to achieve the desired task without having a remote wireless sensor. Harsh environmental conditions that make it difficult to access the sensor combined with limited battery life create a need for wireless sensors to be self-powered. Self-powered systems harvest ambient energy from the environment that would normally be unused. An abundant number of sources for environmental energy exist, including light, air flow, fluidic flow, heat, acoustics, vibrations, and chemical reactions to name a few.

One major challenge in designing a self-powered wireless sensor is to minimize the amount of power required by the system. Minimizing the power requirements is necessary due to limitations on the amount of energy that can be scavenged from any particular environment, as well as the size of the energy collector required to harvest any given amount of energy. For instance photovoltaic solar cells only use about 15% of the energy available from sunlight [1], so to get more electrical energy multiple solar cells must be combined into an array, hence increasing the size of the energy collector. Minimizing the size of the system is important so that the system can be conveniently placed in various remote locations.

The need for low power requirements in a wireless sensor becomes apparent when examining the lifetime of the device. Batteries start to lose their power density over time and must be replaced in order to continue operating the system. Several wireless sensor systems exist that make battery replacement extremely difficult. For instance a wireless biomedical sensor that is implanted under the skin cannot be easily accessed to replace a battery [2]. One option is to use a rechargeable battery, however even rechargeable batteries lose their power density over time, albeit at a much lower rate than standard batteries [3]. Another option for power storage is to use a super-capacitor, which are similar to standard capacitors except with much higher capacitance on the order of a hundred millifarads to several farads [4]. Ultimately the selection of an energy storage device is dependant on the expected lifetime for the final application. This thesis minimizes the average power so that the lifetime of the system can be extended based on the lifetime of the storage device, thus making selection of a storage device much easier.

Most previous work has focused on application specific wireless sensors, and while ultimately the final system tested in this thesis is for a very specific hydrogen sensor the design is extremely flexible so that it can be easily modified to suit any application. While this thesis focuses on the application of a wireless sensor, there are other simple control systems with similar low power constraints that should be looked at for ideas on decreasing the required power. Apart from wireless sensors, simple control systems that gather and utilize data from a sensor are prevalent in everything from digital tire pressure gauges [5] to a new pair of Adidas sneakers that have a built-in microcontroller which uses data from sensors to control the support and cushioning in the shoe [6]. Complete self-powered wireless sensor systems already exist, in particular the MICA Mote [7], and

Smart Dust [8] both of which were developed at UC Berkeley. However these systems incorporate a sensor, control system, and transmitter and therefore are limited to specific applications. Furthermore Smart Dust consists of a custom designed ASIC that integrates the control system with the energy harvesting circuitry. Commercially available wireless sensor systems are on the market. For example, MicroStrain® has two wireless sensor systems which are low power and are small in size: EmbedSense™ which is a passive device that receives power wirelessly and only transmits when queried [9], and StrainLink™ which operates off a battery and still draws power on the order of milliwatts [10]. The design discussed in this thesis will differentiate itself from other designs in that the design will be modular, flexible in its applications, consist of off the shelf components, be able to transmit without querying the system, and maintain ultra-low power requirements on the order of microwatts.

Research Goals

Rather than focusing on addressing the problems related with increasing the amount of available power this thesis focuses on design techniques for minimizing the amount of power required by the wireless sensor system. The main drain on power is the control system which consists of a microcontroller interfaced to a RF transmitter. The microcontroller also provides the interface to the sensor for data collection. The utmost importance is to find a microcontroller that operates at an extremely low power level while also providing the necessary interfaces to sample data from the sensor as well as send data to the RF transmitter.

The goal of this thesis is to design a control system for a self-powered wireless sensor that operates with an average power requirement on the order of a few microwatts. Several techniques for limiting the power consumption of the microcontroller will be

examined including operating the microcontroller at a slower processor speed and using the low power modes available during idle states. Techniques for decreasing the power consumption of the RF transmitter will be examined however the RF transmitter will not be redesigned for this thesis. All parts used in the construction of the control system will be off the shelf components so that reproducibility and ease of reuse is simple.

An additional goal of this thesis is for the control system to be designed with a high level of flexibility, so that the control system does not become application specific. The microcontroller code will be written with variables that are easily modified to change the timing between sampling and transmitting data. The RF transmitter will be a module so that a different transmitter could easily replace the one used without effecting the operation of the system. The microcontroller's sensor interface will be a simple analog to digital converter so that many different sensors can be used. The microcontroller code will be written with a very basic modular structure so that modifying the code to encode or store the data can be done very easily with minor modifications to the code.

Thesis Organization

This thesis is organized into six chapters. This chapter provides background information about wireless sensors as well as providing an introduction to the research goals of this thesis. Chapter 2 reviews the previous work and theoretical information involved with designing a control system for a self-powered wireless sensor. Chapter 3 discusses the actual design process for the control system as well as an introduction to the energy harvesting circuits used. Chapter 4 explains the experimental methods used for testing the components of the control system as well as integrating the system into a self-powered wireless sensor. Chapter 5 discusses the results of testing the control system and the results of the system level testing of the complete self-powered wireless sensor.

Chapter 6 outlines conclusions made from the testing, and provides insight into possible future work to further decrease the power requirements of a self-powered wireless sensor.

CHAPTER 2 THEORETICAL DEVELOPMENT

Background information about self-powered wireless sensors, specifically their control systems is presented in this chapter. Aspects of other people's work in the area of wireless sensors are discussed in this chapter, including the growing amount of research being done on wireless sensors networks. Finally this chapter will review the challenges associated with designing an ultra-low power control system for a self-powered wireless sensor.

Background Information

The simplest form of a wireless sensor is a RF transmitter connected to a data sensor. However a RF transmitter without any control circuitry will continuously transmit. Continuous transmission requires a continuous power source. In order to minimize the average power required a simple control circuit needs to be implemented. The control circuit is used to control the time the transmitter requires power as well as providing an interface between the data sensor and the RF transmitter. The control system also provides the ability to encode the data being transmitted as well as make decisions about transmissions based on the data from the sensor.

A control system cannot be designed without having some knowledge about what is being controlled. In the case of a self-powered wireless sensor, the control system controls the sampling rate of data from the sensor, the frequency of transmission, the data rate to the transmitter, and if any decision making or data encoding needs to be done prior to transmission. The precision level of the microcontroller's interface to the sensor must

be known in order to determine if any external amplification of the sensor's signal is needed. The type of sensor also matters, since passive sensors require a biasing circuit to create a voltage that represents the data value from the sensor. For specific applications a custom microcontroller could be designed to incorporate any extra circuitry needed to interface the specific sensor.

This thesis focuses on the design of a control system which is generic in that it is very flexible and has been designed with a high level of modularity so that the control system can be used in a variety of different wireless sensor applications. Additionally the control system will be designed using commercially available components, so that the design process is simpler and quicker than attempting to design a custom controller. Using off the shelf components also provides a better opportunity for success over a custom controller since the components have already been tested by the manufacturer. Ultimately the techniques used in this thesis to lower the average power of the control system could be applied to custom designed controllers as well.

Previous Work

Over the past decade research in the area of wireless sensors has been growing. The majority of research has been toward creating wireless sensor networks with their own operating systems and communication protocols. In fact, several companies have developed wireless sensor nodes that are specifically designed for use in creating a wireless sensor network. Startup companies like Coronis Systems [11], Dust Networks [12], Crossbow® Technology Inc. [13], and Cirronet, Inc. [14] all have developed wireless sensor networks. Even larger companies such as Intel are researching wireless sensor networks as a potential new revenue stream [15]. With the increasing number of different sensor networks there has been more and more research into the standardization

of communication protocols for wireless sensor networks. The University of California, Los Angeles has developed a sensor network-specific media access control protocol called S-MAC [16]. The goal of S-MAC is to reduce the amount of energy wasted due to constant listening, collisions, overhearing and overhead. A more industry wide standard is IEEE 802.15.4 [17], which defines both the physical and media access control protocols for wireless sensor networks. Several companies have combined to create the ZigBee Alliance [18], which promotes the IEEE 802.15.4 standard. S-MAC and IEEE 802.15.4 are just two of the protocols being developed; other protocols include the use of Bluetooth [19], PicoRadio [20], and various simple RF communications. One of the more interesting ideas is the use of TCP/IP protocol to allow wireless sensor networks to connect to the Internet [21]. Connecting wireless sensor networks to the Internet would allow for remote monitoring from anywhere with Internet access.

One of the main challenges to wireless sensors is maintaining an ultra-low average power consumption. Back in 1995 a group from the University of Michigan designed a low-power wireless sensor system that operating using $700\mu\text{W}$ of power, however the system used a 6V battery and barely made it halfway through a year before needing to replace the battery [22]. Since then the average power of most wireless sensor systems has been targeted at under $100\mu\text{W}$, with most people aiming to reach average power on the order of a few microwatts or less. A variety of techniques for lowering the average power consumption, other than changing the data protocols, have been and are currently being developed. One such technique is designing ultra-low power transmitters, such as the CMOS RFIC being developed by Mohammed Ismail in Sweden [23]. A more common technique for lowering the average power is to build a custom microcontroller.

While custom microcontrollers can operate on less power than most commercial microcontrollers, the design process for generating and testing a custom IC is long and tedious. Furthermore, a corporation that focuses on producing a generic microcontroller that is ultra-low power has an advantage over universities and small groups that try to develop a custom device due to the man power and engineering time available to the corporation.

One of the ultimate goals of low power wireless sensors is to operate off low enough power that the energy required can be harvested through ambient energy sources, thus making the system “self-powered”. Shad Roundy has written a book [24] that focuses on the area of energy scavenging for wireless sensors. Additionally, Shad Roundy has created a 1.9GHz RF transmit beacon [25], that while it does not sense anything and only acts as a transmitter the design operates of environmentally scavenged energy. A group at the University of California, Berkeley has developed a wireless temperature sensor that operates off the vibrations in a staircase [26]. More and more work on the area of self-powered wireless sensors seems to be available everyday as progress in the area continues at a strong and fast pace. This thesis differentiates itself from other work in that the design is modular and focuses purely on techniques for lowering the power requirements of the control system, while using commercially available components.

Design Challenges

Several challenges exist when designing an ultra-low power control system for a self-powered wireless sensor. Minimizing the power consumption is the main challenge in designing a control system for a self-powered wireless sensor. Several aspects of the design must be analyzed to determine methods for decreasing the power required. The

control system can be broken down into a state machine consisting of sampling data, transmitting data, and remaining idle. Figure 2-1 shows a simple state machine that represents the cycle of a control system for a wireless sensor. The duty cycle of each state determines the total amount of power required for each particular state across a single cycle. Each state must be analyzed to determine methods for reducing the power consumption of the system while in the particular state. While most of the challenges have to do with minimizing the power consumption of the control system, other challenges include designing the interface to the sensor and the transmitter as well as determining the format of the data to transmit.

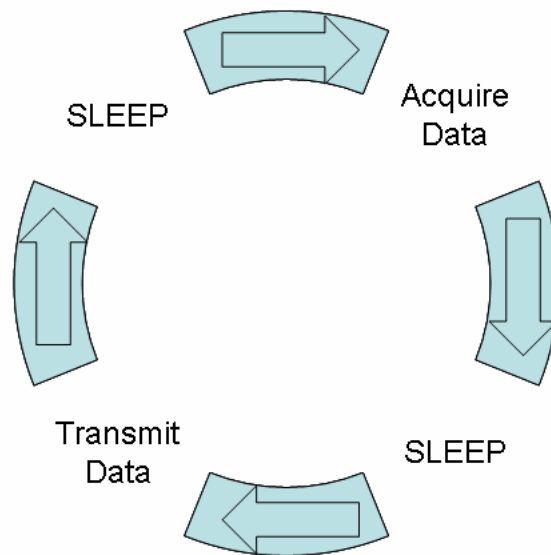


Figure 2-1. Simple state machine of a control system for a wireless sensor.

CHAPTER 3
DESIGN OF A CONTROL SYSTEM FOR A SELF POWERED WIRELESS SENSOR

A self-powered wireless sensor consists of four major components: energy reclamation, data sensor, microcontroller, and a RF transmitter. Figure 3-1 shows a block diagram of the system. Each component has been designed independently however information from the design of each component was taken into account by the other components. This chapter focuses on the design of the control system, which consists of the microcontroller and RF transmitter.

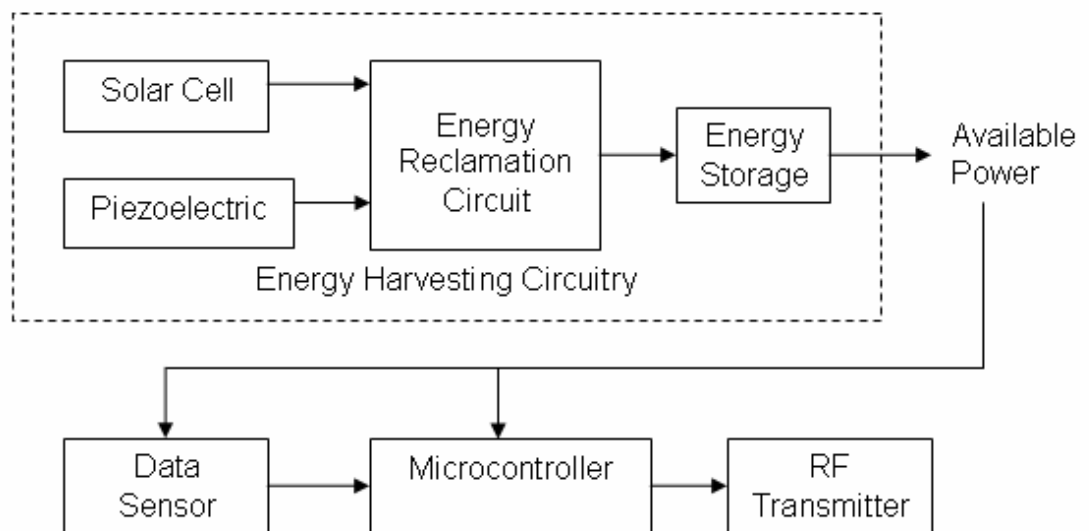


Figure 3-1. System level block diagram of self powered wireless sensor.

Selection of a Microcontroller

When considering a microcontroller it is important to compare several different features. The most important aspect to consider for the application of a self-powered wireless sensor is for the microcontroller to use the least amount of power. The majority of power used is during the microcontroller's active state. However the standby current

is just as important, since the microcontroller will still be drawing power during its sleep mode. The standby current is particularly important since the power source for a self-powered wireless sensor may not be constant. So that power is not wasted on the microcontroller operation, it is desired to have a very short wakeup time. Additionally, to conserve power a low port leakage is desired. A comparison of power characteristics for several microcontrollers is shown in Table 3-1.

Table 3-1. Power characteristics of microcontrollers.

Manufacturer and Model	Active Current	Standby Current	Wakeup Time	Brown-Out Reset	Port Leakage
TI MSP430F1122	14uA@32kHz, 2.5uA@4kHz and 2.2V	4 low power modes from 0.7uA to 0.1uA	6us	50nA	50nA
Microchip PIC16F73	20uA@32kHz	1uA	1ms	85uA	1uA
Motorola MC9S08G	812uA@1MHz	3 Stop modes: from 4.3uA to 25nA	2.4ms	70uA	25nA
Atmel Atmega169	27uA@32kHz	5 Sleep modes, lowest is 0.2uA	10us	19uA	1uA
EM Micro EM6617	9uA@32kHz	0.6uA standby 0.1uA sleep	NA	NA	NA
XEMICS XE88LC01A	10uA@32kHz	1uA in hibernating mode 0.1uA in sleep mode	NA	NA	NA

In order to completely compare the microcontrollers, a comparison of all of the features of the microcontroller is required. For a self-powered wireless sensor the microcontroller must contain an ADC to interface the sensor, a serial output to interface the RF transmitter, and enough memory to hold the runtime code as well as store data from the sensor. A comparison of the features for several microcontrollers is shown in Table 3-2.

Table 3-2. Added features of microcontrollers.

	MSP430	PIC16F73	MC9S08G	Atmega 169	EM6617	XE 88LC01A
Oscillator	1MHz internal, input for 32kHz external	32kHz external	32kHz external	1MHz internal, input for 32kHz external	32kHz crystal	100kHz - 4MHz RC oscillator, 32kHz external
ROM	NA	NA	NA	NA	6kB	22kB, 8kB
RAM	512B-2kB depending on package	192 bytes	1K-4K depending on package	1KB SRAM	(2) 64x4 bit	8 bytes low-power RAM, 512 bytes
E ² PROM	NA	NA	NA	512 bytes	64x8 bit	NA
ADC	8-channel 12-bit	5-channel 8-bit	8-channel 10-bit	8-channel 10-bit	2-channel 8-bit	16 +10 bit Zooming ADC
UART	2 USART	USART	NA	Serial	NA	Serial UA
I/O Ports	48 I/O lines	22 I/O lines	34-56 I/O lines depending on package	53 general purpose I/O lines	(1) 4-bit input, (2) 4 bit bi-dir, (1) serial write buffer	24 I/O lines
FLASH	16kB - 60kB depending on package	4Kx14 bit	16K-60K depending on package	16KB	NA	NA

In terms of features, all of the microcontrollers have adequate features for the design of a self-powered wireless sensor. From the power characteristics listed in the Table 3-1, the MSP430, EM6617, and XE88LC01A look like clear favorites (all are around 10 μ A active current down to 0.1 μ A sleep mode current). However neither the EM6617 nor XE88LC01A have given data for port leakage or wakeup time. The final decision was to go with the TI MSP430 since it has an abundance of available resources and since TI gave samples and offered support.

Design of Programming Code

The code for the microcontroller is designed with flexibility in mind. This is done so that the design can be tailored to any specific application with minimal code redesign required. Along those same lines two different versions of code were written. Each version of code presents a slightly different mode of operation. The two modes of operation are listed below.

1. Level Monitoring. Constantly monitors sensor and sends a single emergency RF pulse when the sensor's data goes above a given threshold value.
2. Data Transmitting. Constantly monitors sensor and sends data every given number of seconds. The delay is overridden if the sensor's data goes above a given threshold value.

The program code was written in the C programming language. The C code for both modes of operation is given in Appendix A. Regardless of the mode of operation, the structure of the code is very similar. The microcontroller code is broken into two main sections: initialization and interrupt routines. This allows the microcontroller to constantly be in a sleep mode with the CPU turned off, functioning in an interrupt driven architecture.

The initialization section is common for both modes of code. The sampling delay is defined in the initialization section as CCR0. CCR0 is defined in terms of a number of 32 kHz clock cycles. For example, if CCR0 is set to 500, then the delay equals 500 divided by 32 kHz or about 15 ms.

The interrupt routines consist of a timer interrupt and an ADC interrupt. The timer interrupt is used to initiate ADC samples, as defined by the amount of time CCR0 is set to in the initialization section. The ADC interrupt occurs once an ADC sample has been

taken. The ADC interrupt is used to determine what if anything to send out over the RF transmitter.

Level Monitoring

For the case of level monitoring the microcontroller conserves power by only transmitting a signal when the sensor's data goes above the threshold value. The microcontroller runs a very basic state machine consisting of the following states: initialization, collect data, analyze data, transmit data, and sleep. A timer is used to delay sampling the sensor data. A basic flow chart of the microcontroller's state machine is shown in Figure 3-2.

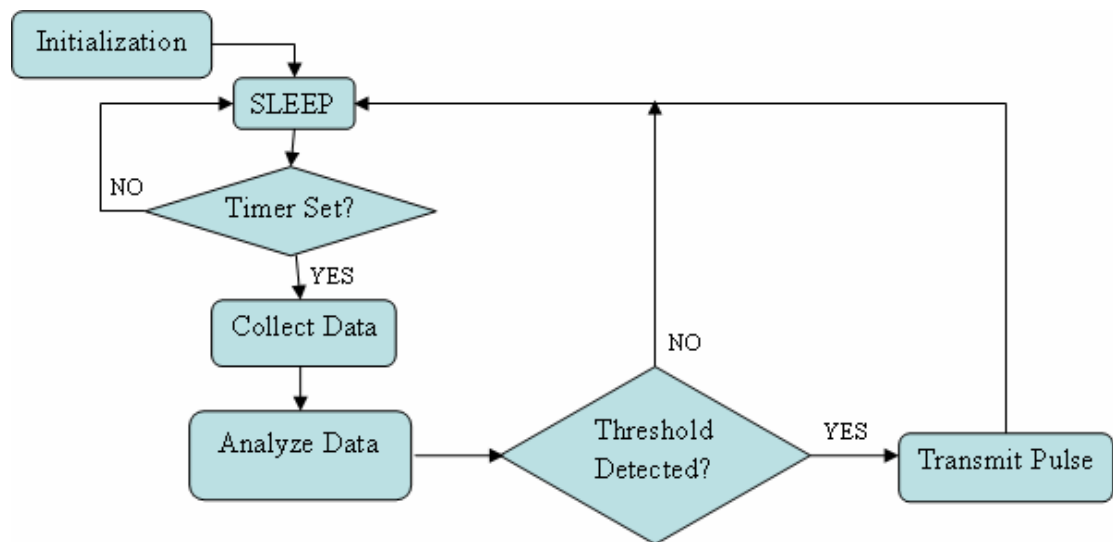


Figure 3-2. Microcontroller flow chart for level monitoring.

The state machine is designed to run using a single timer to cycle through sampling data and sleep mode. However if the data is above a threshold value then the microcontroller immediately sends a single RF transmission and resets the timer. One foreseen problem is that when the sensor's data is above the threshold value the control system will constantly be transmitting until the sensor's data drops below the threshold value. The solution to this problem is to use a static variable that is set in the code once a

transmission occurs. This variable gets cleared when the sensor's data falls back below the threshold level.

The case of level monitoring has two settings that can be modified: threshold value and transmit pulse length. The ADC sample is examined in the line “if (ADC10MEM < 0x1FF)” where 0x1FF is the threshold value. Since the ADC sample is 10 bits the maximum value is 0x3FF and the minimum is 0x000, so 0x1FF is halfway between the two. The threshold value is defined as a function of the supply voltage, so for a 2 V supply voltage each bit is equal to $2 \text{ V} / (2^{10}) = 1.95 \text{ mV}$. For the case of a sensor that needs to be monitored for a falling voltage level, the code can be modified so that the comparative statement is “if (ADC10MEM > 0x1FF).” The data pulse is defined as just a single voltage pulse on the data line to the RF transmitter. The length of time the data line is held high is defined by the variable *pulse_length*, which is defined in terms of a number of 32 kHz clock cycles. The shorter the length of the pulse the less average power the system takes, as the pulse is used to turn on the RF transmitter.

Data Transmitting

For the case of data transmitting, the microcontroller cycles between sampling data and transmitting the data. The microcontroller runs a very basic state machine consisting of the following states: initialization, collect data, analyze data, store data, transmit data, and sleep. The state machine is designed to run using timers to add delays between collecting data and transmitting the data. However if the data is above a threshold value then the microcontroller immediately sends a single RF transmission and resets the timers. The code has the same foreseen problem as the level monitoring code, that when the sensor's data is above the threshold value, the control system will constantly be transmitting until the sensor's data drops below the threshold value. The same static

variable solution from the level monitoring code is used for the data transmitting code. A basic flow chart of the microcontroller's state machine is shown in Figure 3-3.

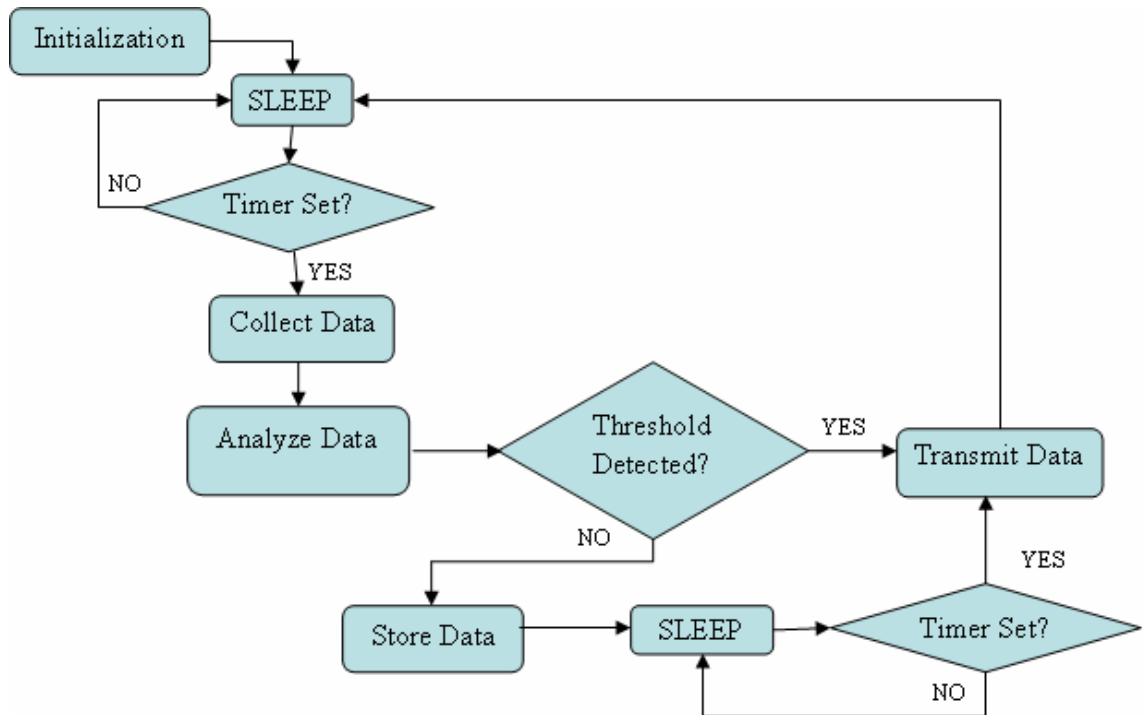


Figure 3-3. Microcontroller flow chart for data transmitting.

The case of data transmitting has three settings that can be modified: transmission delay, transmitted data, and threshold value. The threshold value is defined similarly to the threshold value for the level monitoring code. The transmission delay is defined by the variable *transmit_dly*, which is defined in terms of a number of 32 kHz clock cycles. The transmitted data is currently defined simply as the sampled ADC value, where each bit represents 1.95 mV for a 2 V supply voltage. This is the simplest method for saving processing power, however once a sensor is chosen a coding scheme can be defined that would decrease the number of bits needed to transmit, and hence decrease the amount of power even further.

Programming Techniques for Minimizing Power Consumption

One of the keys to minimizing power consumption is to put the microcontroller in a sleep mode for as long as possible. The MSP430 has 5 modes of operation: Active Mode and Low Power Modes 0-4 (LPM0-LPM4). As the level increases from LPM0 to LPM4, the amount of the microcontroller that is active decreases. The CPU portion of the microcontroller is turned off in all low power modes. The peripherals like the ADC and USART can be enabled and disabled individually. By individually enabling and disabling the peripherals as they are needed power is not wasted on inactive portions of the microcontroller.

Another method for decreasing the amount of power consumed by the microcontroller is to decrease the clock frequency. The MSP430 has an internal 1MHz clock, however the microcontroller can be operated using an external 32 kHz crystal oscillator. Both the ADC and USART can be operated off the 32 kHz oscillator, which means the 1 MHz built in clock can remain off at all times except during initialization. Using an external clock allows the MSP430 to run in LPM3 which is the second lowest low power mode. The datasheet for the MSP430 [27] gives the following equation that correlates how the current consumption changes as the clock frequency changes.

$$I(\text{AM}) = I(\text{AM})_{[1 \text{ MHz}]} \times f(\text{System}) [\text{MHz}] \quad (3.1)$$

Where $I(\text{AM})$ is the current for active mode operation, $I(\text{AM})_{[1 \text{ MHz}]}$ is the current for active mode operation at 1 MHz, and $f(\text{System})$ is the operating frequency. The equation shows a linear relationship between the current consumption and the operating frequency. According to the datasheet the current consumed at 1 MHz is 500 μA , thus the equation can be simplified to

$$I(\text{AM}) = (500 \mu\text{A} / \text{MHz}) * f(\text{System}) \quad (3.2)$$

Figure 3-4 shows a graphical representation of the current consumption versus frequency, for a supply voltage of 3 V.

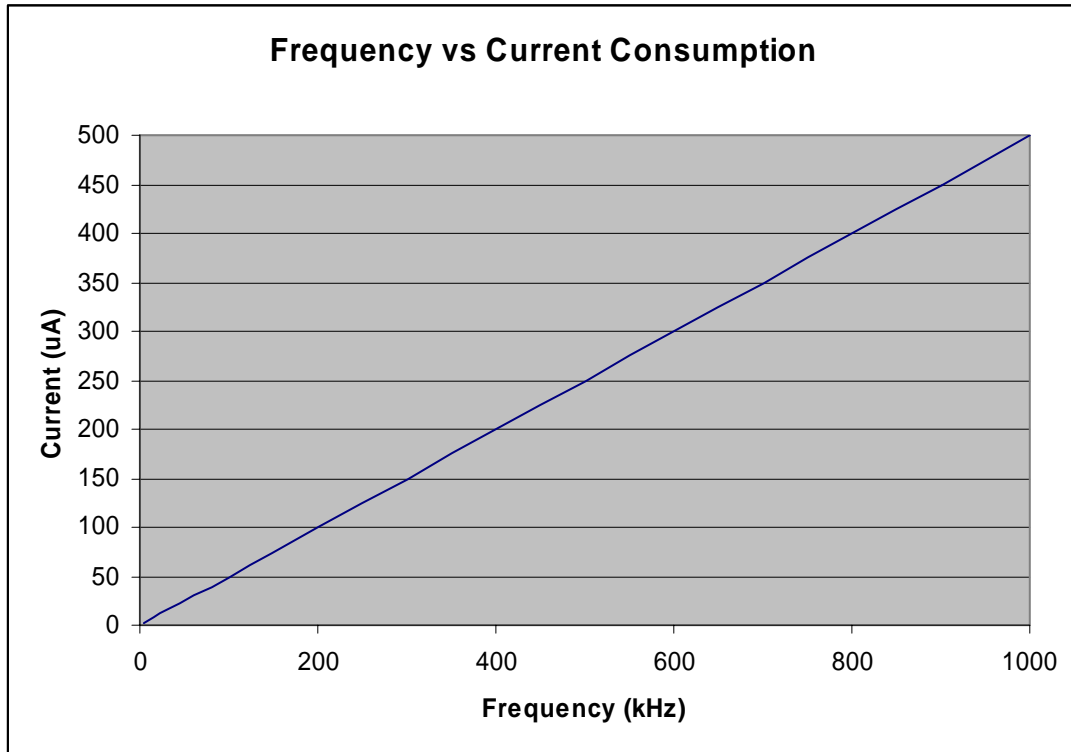


Figure 3-4. Frequency versus current consumption for MSP430 operating at 3V.

The next major way to decrease the power consumption for the microcontroller is to decrease the supply voltage. The microcontroller can operate with a supply voltage between 1.8 V and 3.6 V. The MSP430 datasheet provides the following equation that correlates the supply voltage to the current consumption based on a 1 MHz operating frequency.

$$I(\text{AM}) = I(\text{AM})_{[3\text{V}]} + 210 \mu\text{A}/\text{V} * (V_{\text{CC}} - 3 \text{ V}) \quad (3.3)$$

Where $I(AM)_{[3V]}$ is the current consumption when operating at 3 V and V_{CC} is the supply voltage. This equation provides a linear relationship between supply voltage and current consumption and is shown graphically in Figure 3-5.

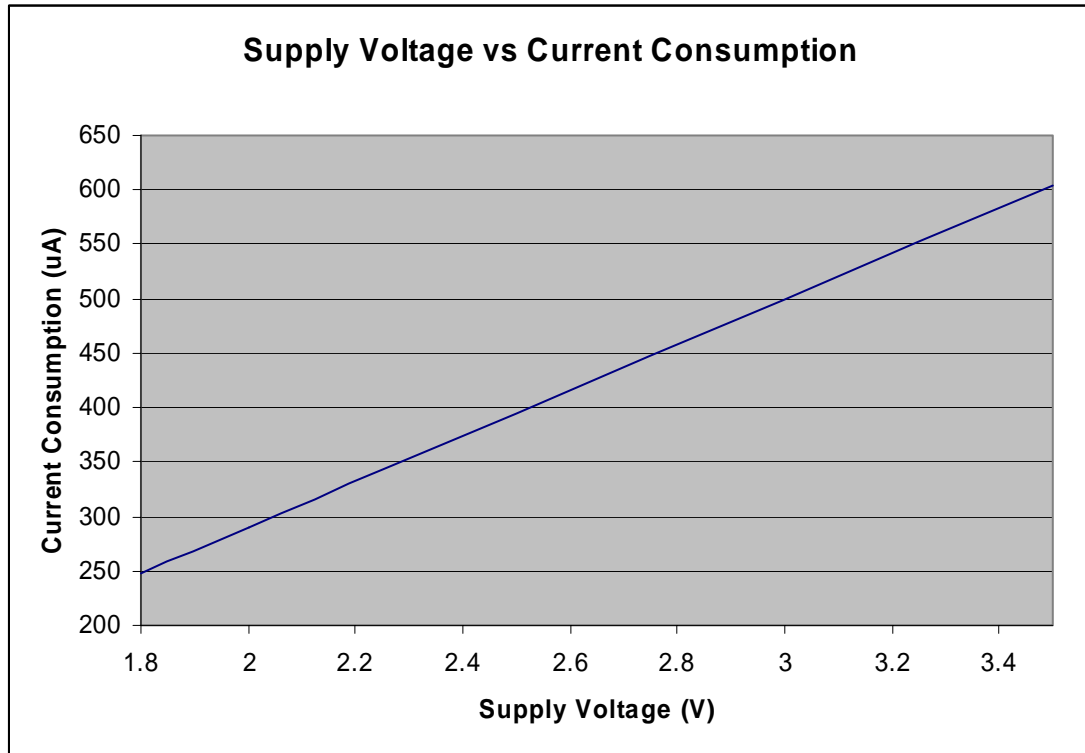


Figure 3-5. Supply voltage versus current consumption for MSP430 operating at 32 kHz.

The original design for the programming code involved using the UART to serially transmit data to the RF transmitter. Even with the ability to enable and disable the UART around a sleep cycle, the default value being output on the UART was a “1”. With the UART outputting a “1” the RF transmitter would be transmitting a “1” which would be a waste of power. In order to minimize the power, the code was re-written to use a single output port of the microcontroller and simply serially shift the data bit by bit to RF transmitter. One additional benefit of using an output port instead of a UART is that the data pattern does not have to follow the parameters defined for a UART. Having open

options for the data pattern means that the data can be any length and can be as many or as few bits as desired.

RF Transmitter

The used of a RF transmitter is required to wirelessly transmit the data from the sensor. An RF transmitter has several design considerations such as transmission frequency, transmit distance, data rate, and power usage. The power usage is the most important of these design criteria in the design of a self-powered wireless sensor. However the transmit distance has a minimal length to be useful. Thus the design needs to be optimized for lowest possible power for a useful transmission distance.

Design of RF Transmitter

RF transmitters typically consist of four parts: frequency determining device, amplifier, feedback circuit and output. A relatively simple design is the key to keeping the RF transmitter's power usage low. Obviously the fewer active components in a design the less power that is required. The simplest form of a frequency determining device is a LC oscillator. The LC oscillator uses an inductor and a capacitor to provide initial oscillations. The resulting oscillation of the inductor and capacitor is then input into an amplifier via a feedback circuit. The amplifier then provides the amplified oscillating signal to the output. The following simple formula is used to determine the oscillation frequency based on the values of the inductor and capacitor.

$$f_r = \frac{1}{2\pi\sqrt{LC}} \quad (3.4)$$

A Colpitts Oscillator is an example of a circuit design that employs a LC oscillator and is a prime candidate for a very simple RF transmitter. The Colpitts Oscillator consists of a LC oscillator along with a single transistor acting as a unity amplifier and

feedback circuit. Ming Microsystems Inc. has fabricated a RF Transmitter (TX-99) based on the Colpitts Oscillator design. Figure 3-6 shows the schematic for the TX-99. The datasheet [28] provides full operational details for the TX-99.

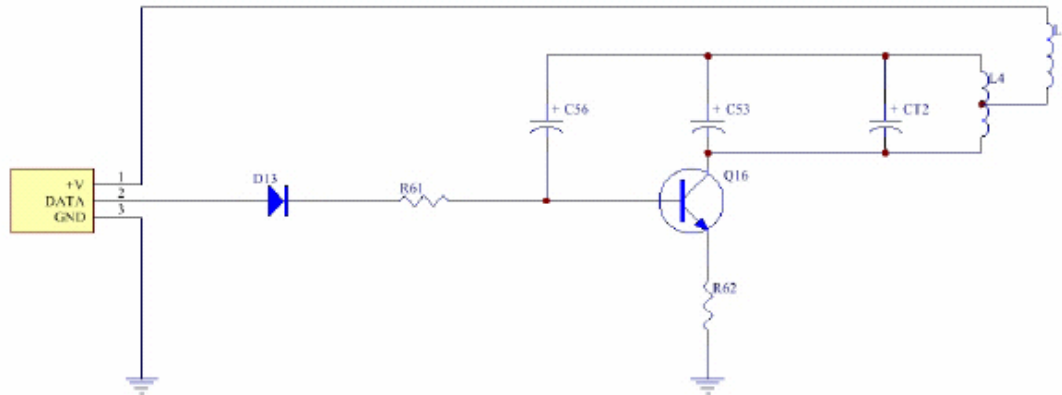


Figure 3-6. Schematic of TX-99 RF transmitter.

Power Consumption for a RF Transmitter

The power required for data transmission depends on the transmission distance, transmission frequency, and the data rate. There are two methods for estimating the power required for RF transmission: Free Space and Plane Earth. The Free Space method assumes unobstructed transmission in all directions. The Plane Earth method takes into account that the transmission is done on a plane and hence depends on the height of the transmitter and receiver above the plane.

Free Space method

The Free Space method yields the following equation [29] relating the power loss to the transmission frequency and the distance between transmitter and receiver, assuming a dielectric constant of 1.

$$\text{Power Loss} = 20 \cdot \log(4 \cdot \pi \cdot D \cdot f / c) \quad (3.5)$$

Where D is the distance between the transmitter and receiver, f is the frequency, and c is the speed of light. Power loss is defined as the difference in the power of the transmitted signal between the transmitter and the receiver. A receiver requires the transmitted signal to have some minimum amount of power, in order to interpret the signal. Hence the minimum power required for transmitting is primarily dependant on the minimum amount of power required in the transmitted signal at the receiver. The frequency of the transmission and the distance between the transmitter and receiver add to the total power required for transmitting. Figure 3-7 shows a plot of transmission distance versus power loss for given frequencies.

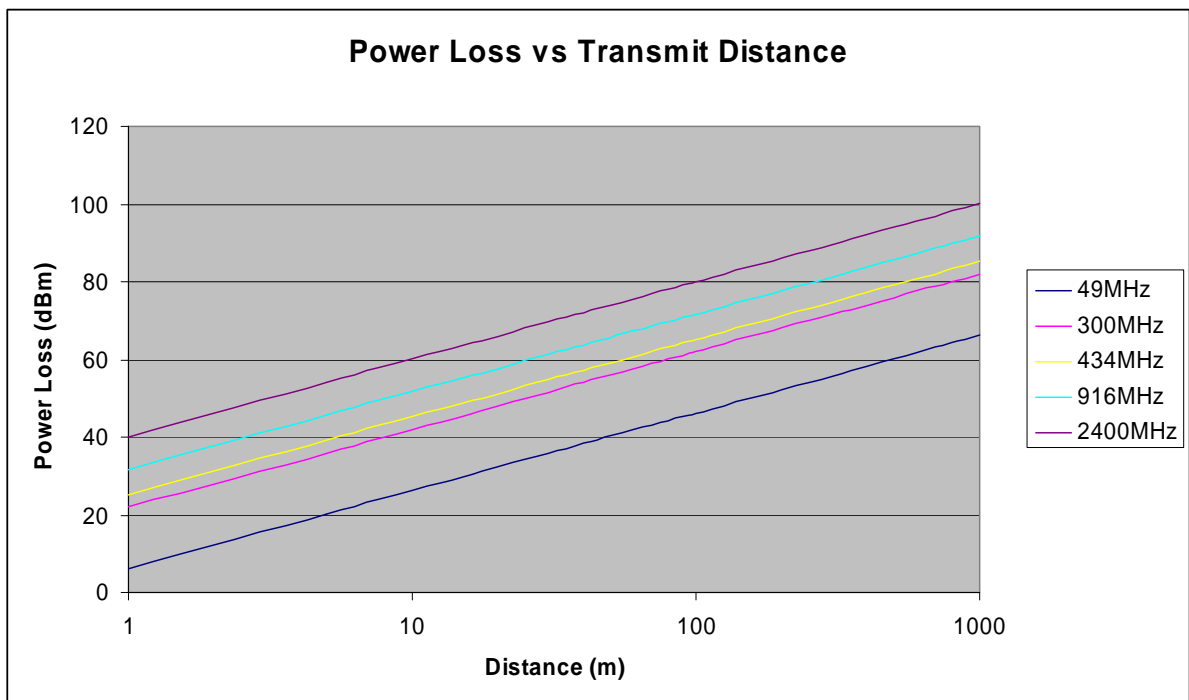


Figure 3-7. Transmission distance versus power loss for given frequencies.

As the transmission frequency decreases, the power loss for a given distance decreases. Similarly for a given frequency, as the distance between transmitter and receiver increases the power loss increases. Thus, to minimize the amount of power lost

in transmission, and hence minimize the amount of power required for transmitting, a low frequency is desired.

Plane Earth method

The Plane Earth method takes into account the height above the Earth of the transmitter and receiver. One benefit of reviewing the Plane Earth method is that the equation that describes power loss is valid for an entire frequency band. Removing the dependence on frequency provides an equation that only depends on the geometry of the distance between the transmitter and receiver. According to the Plane Earth method the following equation is valid for frequencies in the UHF band (300 MHz to 3 GHz).

$$\text{Power Loss} = 20 \cdot \log[D^2 / (H_T \cdot H_R)] \quad (3.6)$$

Where D is the distance between the transmitter and receiver, H_T is the height of the transmitter, and H_R is the height of the receiver. The above equation makes it obvious that as the distance between the transmitter and receiver increases the power loss increases, however as the height above the ground of the transmitter and/or receiver increases the power loss decreases. Thus, one method for minimizing power would be to increase the height of the transmitter and receiver. A graphical representation of the Plane Earth equation for power loss is shown in Figure 3-8.



Figure 3-8. Power loss vs. transmit distance for various transmitter and receiver heights.

Techniques for minimizing power consumption

From the Plane Earth and Free Space methods, the obvious ways to minimize power consumption are to use a low frequency and to increase the height of the transmitter and receiver. In terms of the operation of the transmitter, one method for lowering the required power is to use On/Off Keying (OOK) which synchronizes the power supplied to the transmitter with the data being supplied. Compared to other methods such as Frequency Shift Keying (FSK), OOK transmitters are simpler, require at least 50% less transmitter current, and require less bandwidth [30]. The control system designed for this thesis uses the OOK method by connecting the output port of the microcontroller to both the data and supply voltage inputs of the transmitter. Thus the transmitter is only powered when it is transmitting a “1.”

Another method for reducing the power is to decrease the number of bits transmitted per transmission. However the number of bits transmitted depends on the end application for a wireless transmitter and what information is desired to be transmitted. Similarly, the number of transmissions per second directly effects the amount of power required. The following equation correlates the number of transmissions per second to the average power consumed by the system every second.

$$P_{avg} = [P_{uC} * (1 - (t_{tx} * N_{tx})) + P_{tx} * t_{tx} * N_{tx}] \quad (3.7)$$

Where P_{uC} is the power consumed by the microcontroller, t_{tx} is the time for a single transmission, N_{tx} is the number of transmissions per second, and P_{tx} is the power required for a single transmission.

Construction of a Prototype

A prototype for the control system described in this thesis is constructed using a double-sided copper clad printed circuit board (PCB). Protel software [31] was used to design the electrical schematic and mechanical layout for the PCB as shown in Figure 3-9, Figure 3-10, and Figure 3-11. An LPFK [32] computer-controller surface milling machine was used to etch the design into the circuit board. The layout is designed on both sides of the PCB; one side contains the electrical components and the other side has connectors to interface the various components of the prototype. BNC connectors are used to interface the power source, data sensor, and RF transmitter to the microcontroller. A 14 pin header is used for programming the microcontroller via the microcontroller's JTAG pins. The electrical components consist of the microcontroller, a crystal oscillator, a 50 k Ω resistor used to pull the reset pin of the microcontroller to V_{cc} , and filter capacitors as recommended by the MSP430 datasheet. A photograph of the prototype

with the RF transmitter is shown in Figure 3-12. The photograph shows the bottom side of the board, which contains the interface connectors. The microcontroller and other electrical components are on the top side of the board and are shown in Figure 3-13.

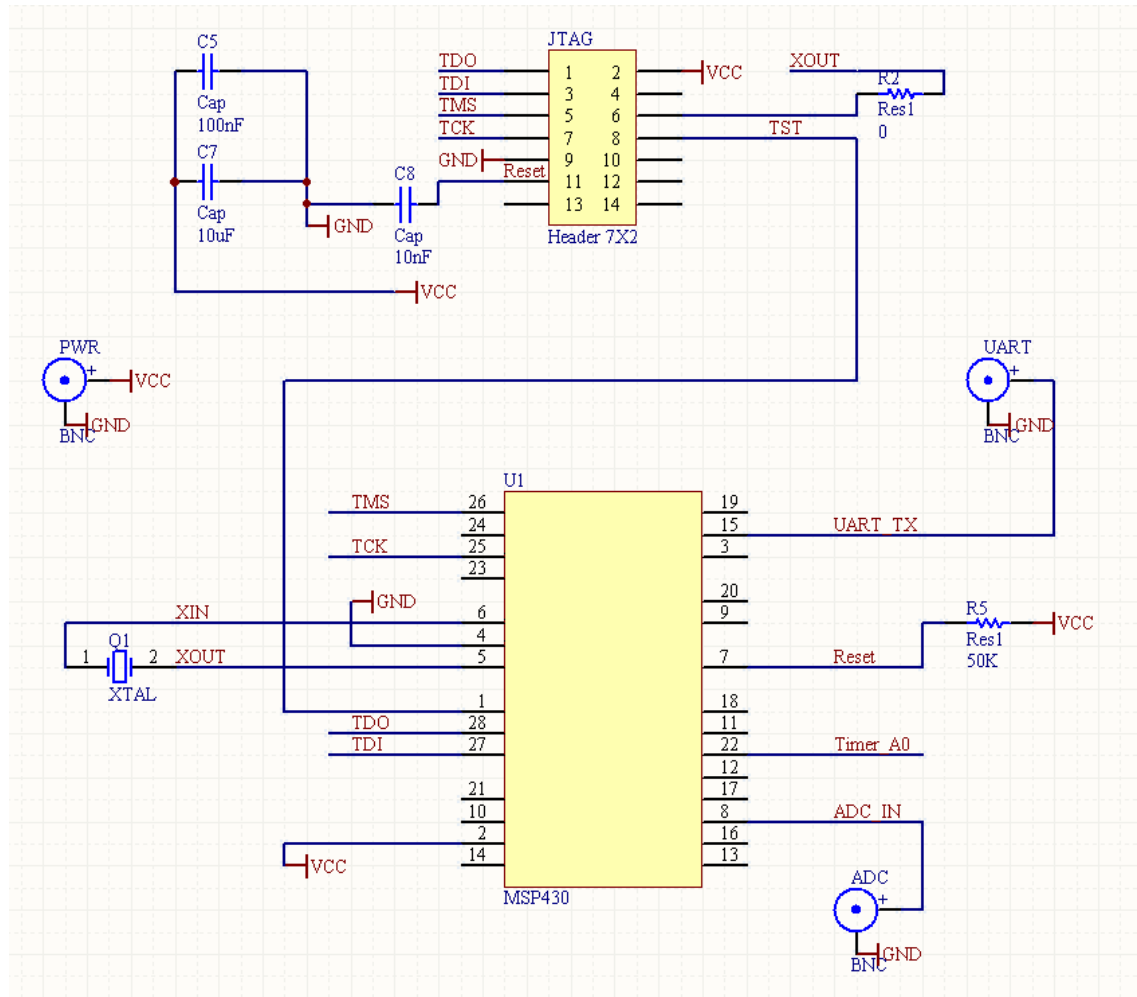


Figure 3-9. Schematic for control system prototype.

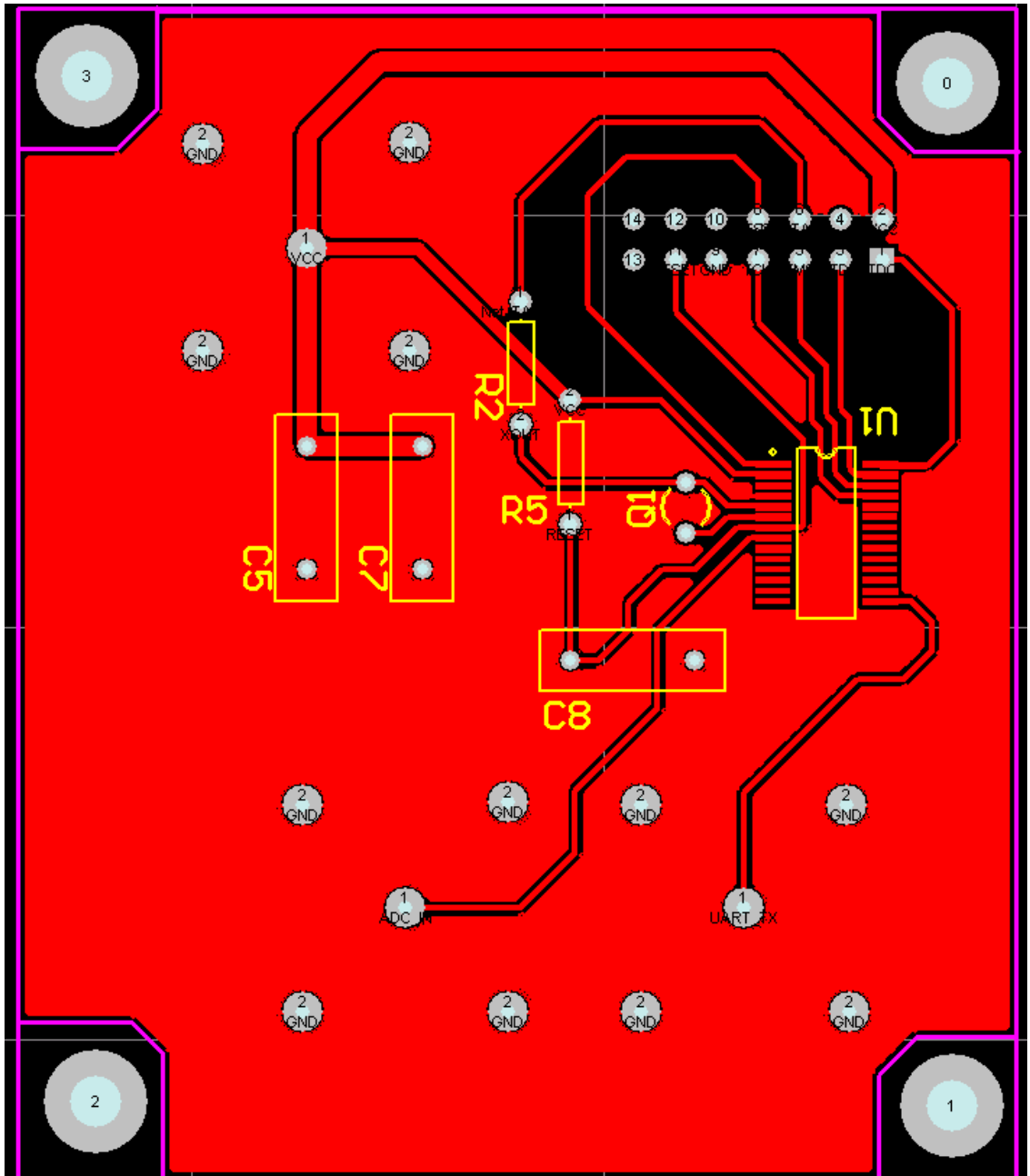


Figure 3-10. Top side PCB layout for control system prototype.

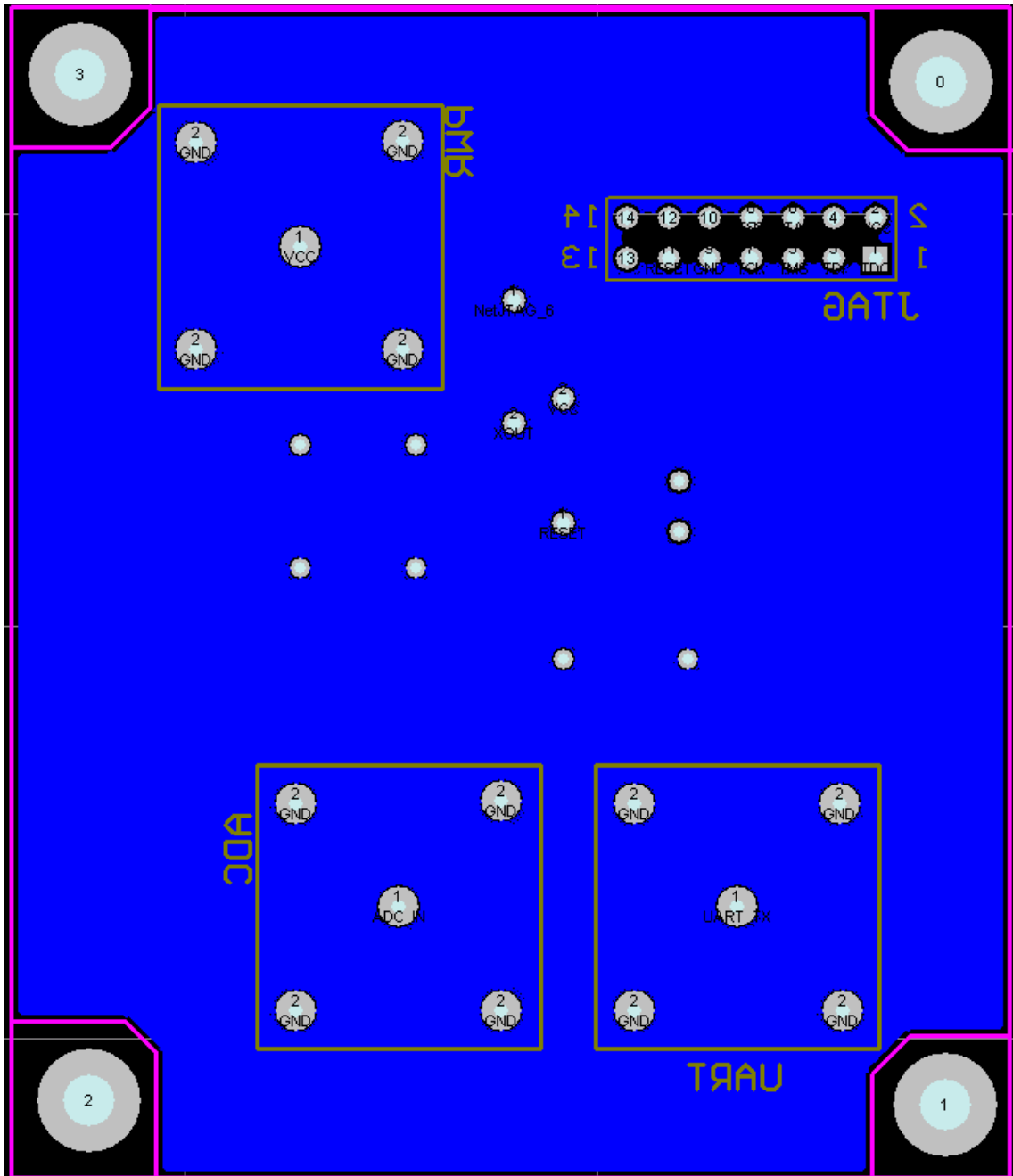


Figure 3-11. Bottom side PCB layout for control system prototype.

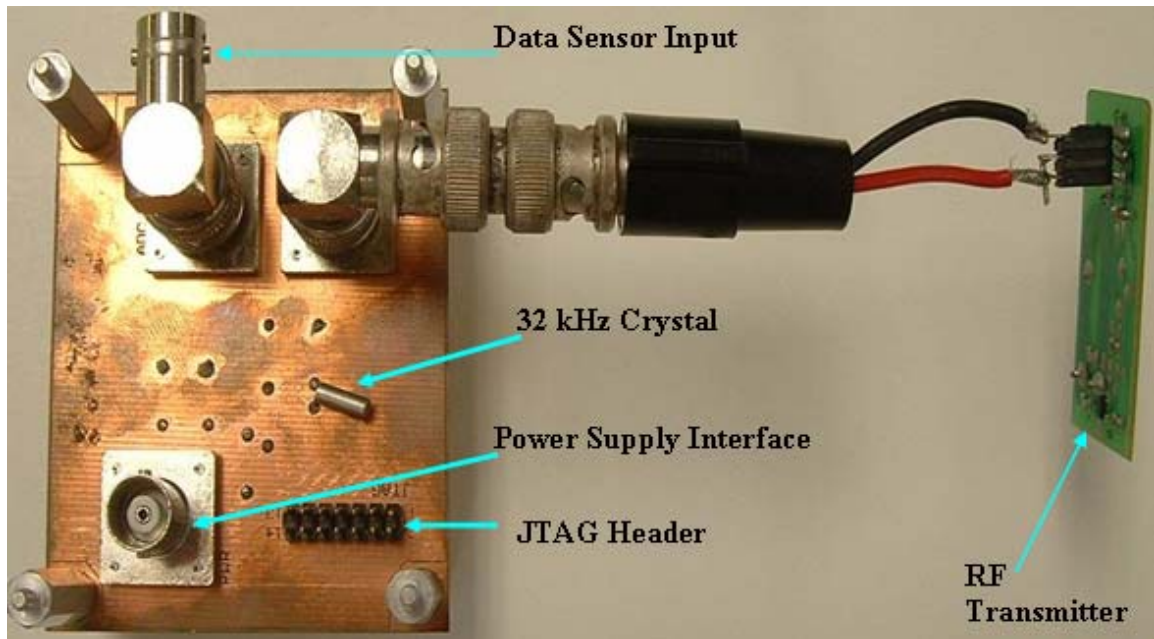


Figure 3-12. Control system prototype with RF transmitter.

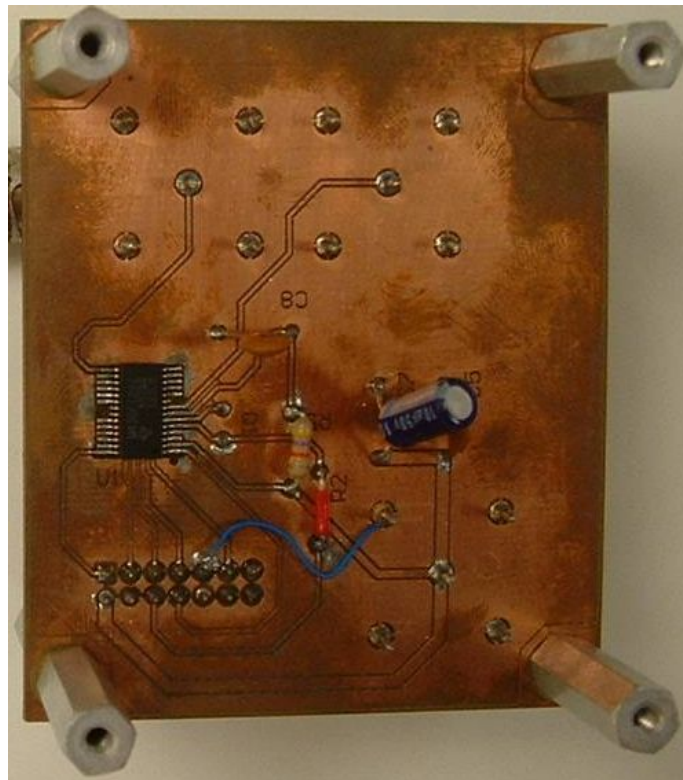


Figure 3-13. Top side of control system prototype.

CHAPTER 4 EXPERIMENTAL METHODS AND SETUP

Testing of a control system for a self-powered wireless sensor consists of testing and verification of the control system as well as testing the control system integrated with the rest of the self-powered wireless sensor. Before integrating the control system with the rest of the self-powered wireless sensor, the energy sources and data sensor must be designed and tested. This chapter gives an overview of the experimental methods and setup required for testing the control system, as well as describing the energy sources and the data sensors used in testing.

Energy Sources

A self-powered wireless sensor must get its power from environmentally scavenged energy. Environmental energy sources include light, wind, heat, vibrations, and the flow of water. Light and vibrations are the two sources that are focused on in this thesis. The reasons for choosing those two sources are the availability of energy conversion devices, the ability to replicate and control the sources, and the various locations where these energy sources are available.

Energy from Light

One of the most readily available environmental sources of energy is the sun. Solar energy is a common energy source used in a wide range of applications from small handheld calculators to traffic signals. Solar cells are used to convert energy from light to electrical energy. The size and efficiency of the solar cell determines the amount of electrical energy available for any given amount of light. Due to the typical constraints

on the size of a wireless sensor, a solar cell used for a wireless sensor needs to be small and highly efficient. IXYS Semiconductor makes a 6mm x 6mm monocrystalline high efficiency solar cell with their part number XOD17-04B [33]. The XOD17-04B solar cell has an open circuit voltage of 630 mV and a short circuit current of 12 mA. In order to attain a higher open circuit voltage multiple solar cells are connected in series. A circuit designed by Shengwen Xu [34] is used to transfer the energy from the solar cell into a storage capacitor that is used to provide the power to the control system. Details of the circuit are shown in the conference paper by Shengwen Xu [34].

Energy from Vibrations

Vibrations are a common source of environmentally reclaimed energy. The use of piezoelectric materials to convert vibrations to electrical energy is widespread [35]. Selecting a piezoelectric material is dependant on several criteria, specifically vibration frequency, efficiency, size and scalability, and magnitude of vibration. Since this thesis focuses on a control system for an ultra-low power wireless sensor, the selection of a piezoelectric is based primarily on size and efficiency. Piezo Systems, Inc. makes a Double Quick Mounted Y-Pole Bender, D220-A4-203YB [36]. This bimorph beam consists of two parallel connected 1.25" x 0.25" x 0.02" pieces of 5A4E piezoceramic [37] on an Aluminum beam. Four of these bimorph beams are mounted on a shim which is connected to an impedance head, as shown in Figure 4-1. A simple direct charging circuit, shown in Figure 4-2, is used to store the energy reclaimed from the beams. The circuit consists of four Fairchild Semiconductor BAT54 Schottky diodes, a 330 μ F electrolytic capacitor and a Panasonic VL1220 2V battery. The four bimorph beams

were connected in parallel to the input of the circuit, in order to maximize the input current.

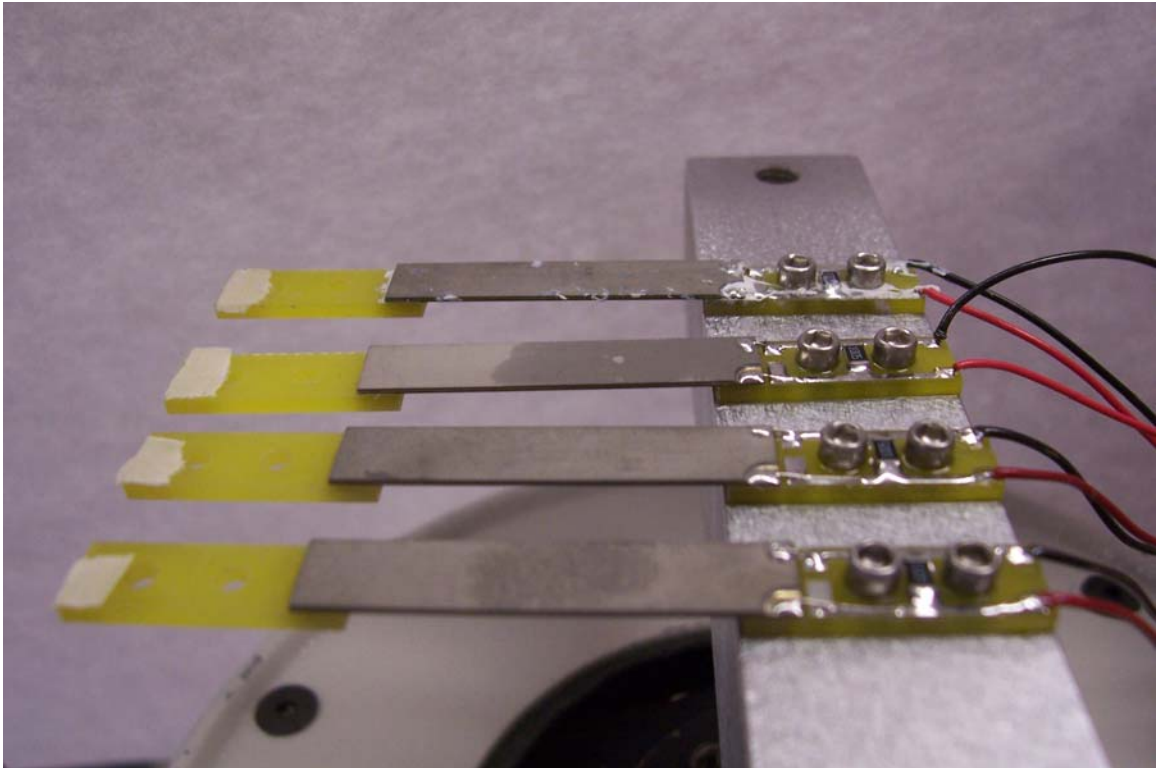


Figure 4-1. Bimorph PZT composite beams.

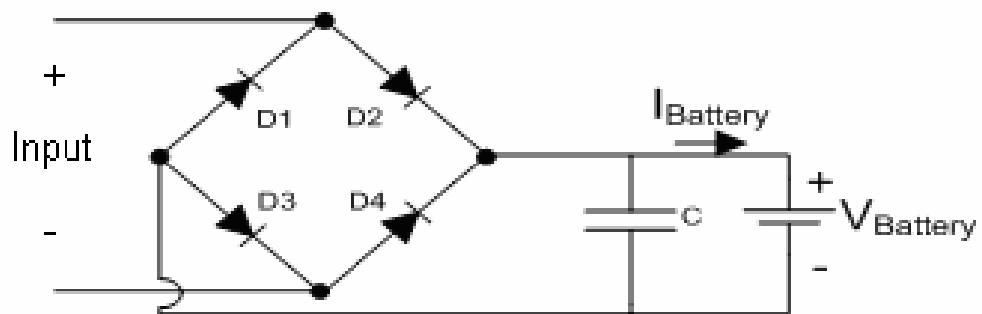


Figure 4-2. Direct charging circuit for energy reclamation from vibrations.

Data Sensor

The microcontroller used in the control system requires an analog voltage as the input for the sensor. This means that any type of data sensor used with the control system must either vary voltage in accordance with what the sensor is sensing, or have some

circuitry that converts the output of the sensor into an analog voltage. To control the voltage of the sensor during initial testing a simple reference voltage supply is used as the data sensor input. Once the control system's functionality is verified a solar cell is used as the data sensor input. A solar cell is used as an example of a sensor that provides a varying voltage as the medium it is sensing changes (in this case as the amount of light shined on the sensor varies). The final sensor that is tested is a hydrogen sensor.

The hydrogen sensor is made of a layer of ZnO nanowires with palladium deposited on top. The sensor acts like a variable resistor, where the resistance changes with respect to the concentration of hydrogen. A characterization of the sensor is required in order to determine how to interface the sensor with the microcontroller. Details about the sensor including a characterization of the sensor are written in several papers [38]. Since the sensor acts like a variable resistor a biasing current is required in order to get a voltage to input to the microcontroller. The design of a biasing circuit was done by Jerry Jun. A schematic of the biasing circuit is shown in Figure 4-3. A photograph of the biasing circuit with an encased hydrogen sensor is shown in Figure 4-4. The biasing circuit requires two hydrogen sensors, one encased and the other open to the environment. The encased sensor provides a fixed resistance to compare to the data sensor's resistance, which is needed since the resistance value can change with variances in temperature as well as hydrogen concentrations. Using two sensors provides a differential voltage, which is amplified before being input to the microcontroller.

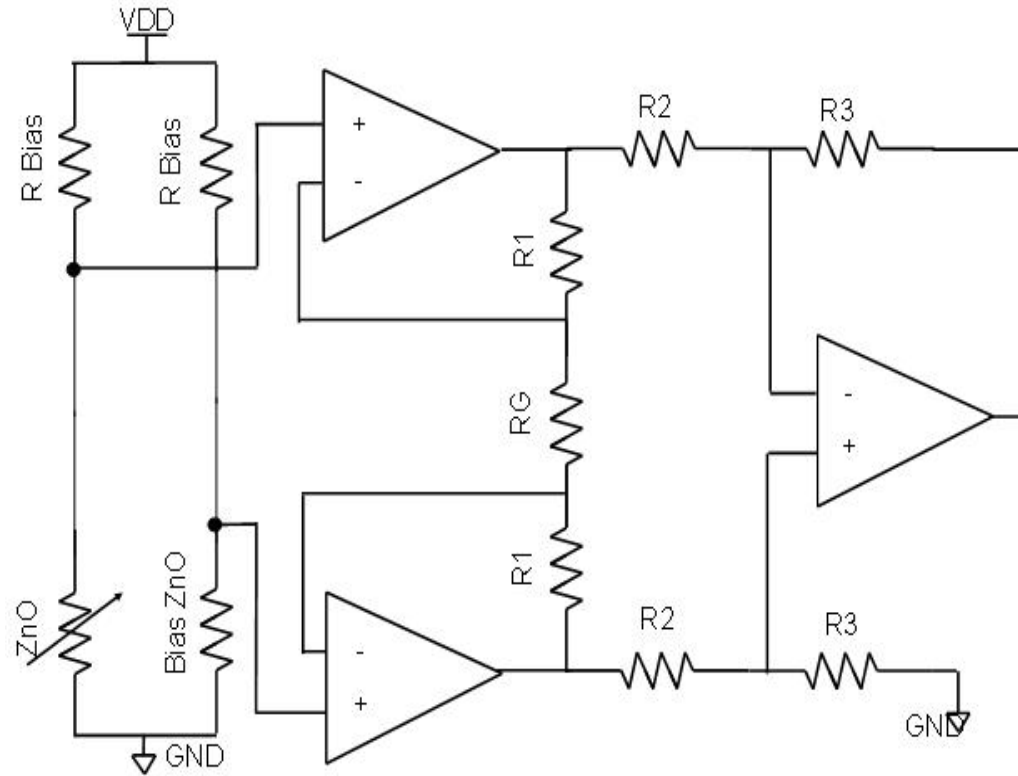


Figure 4-3. Schematic of biasing circuit for hydrogen sensor.

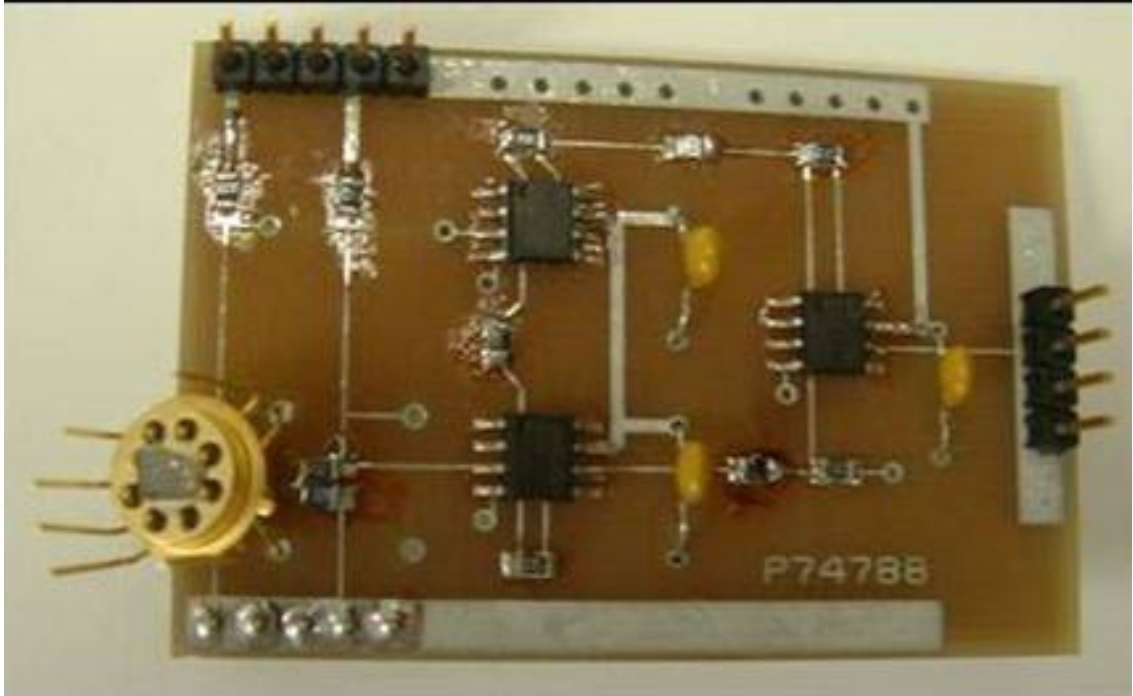


Figure 4-4. Picture of biasing circuit with hydrogen sensor.

Testing Methodology for the Control System

The control system consists of the microcontroller and the RF transmitter, as described in the previous chapter. The focus of the testing of the control system is to determine the power required and to verify the functionality of the system. To verify the functionality of the system, a regulated voltage supply is used as the source of power. By using a regulated voltage supply, the supply voltage is constant and a small series resistor is used to measure the input current and thus determine the input power.

Methods for Measuring Power Consumption

Measurements are taken to assess the power required to sense data, transmit data, and remain idle. All power measurements are done using a Tektronix TDS5104B digital phosphor oscilloscope; this provides a visual display of the power over a period of time. Using an oscilloscope also provides a method for determining peak power, average power, and total energy. A Tektronix P6248 differential probe connects to the

oscilloscope to measure the voltage drop across the series resistor, between the output of the power supply and the input of the microcontroller. A differential probe is used to isolate the grounds between the oscilloscope and the control system.

A small valued resistor is optimal to minimize the effects of the voltage drop across the resistor on the control system. However, too small a value and the voltage drop will be in the noise region of the oscilloscope. From experimentation with various resistor values, the value of 383 Ohms was determined to be optimal for measurements.

The transmitted data can consist of different patterns depending on whether a pulse is transmitted or if a data pattern is transmitted. Several measurements are needed to determine the power required to transmit data. These measurements include the power to transmit: a single pulse, a pattern of all 1's, a pattern of all 0's, and a pattern of mixed 1's and 0's.

Methods for Characterizing RF Transmission

A characterization of the RF transmission is required to determine the maximum transmission distance, the received power, and the frequency spectrum of the received signal. An Agilent E4448A PSA series spectrum analyzer is used to measure the frequency spectrum and the received power. A $\frac{1}{4}$ wave whip antenna made from 22 gauge copper wire is soldered to a SMA connector which attaches to the spectrum analyzer. A picture of the antenna is shown in Figure 4-5. Similar antennas are attached to the transmitter and receiver to determine the additional transmission distance due to the use of antennas. A Tektronix TDS210 two channel digital real-time oscilloscope is used to view the data at the receiver to verify that it matches the data being transmitted. The maximum transmission distance is determined by when the signal at the receiver no longer matches the signal at the transmitter.



Figure 4-5. Whip antenna.

The test setup requires a fixed power supply for the control system as well as a fixed power supply for the receiver. A power source for the spectrum analyzer and oscilloscope is also required. Due to the need for multiple power sources, and the measurements being done over a distance, there are limitations on where the measurements can be taken. The atrium area of the New Engineering Building (NEB) at the University of Florida is where the measurements are taken. Figure 4-6 shows a floor layout of the atrium where the testing takes place.

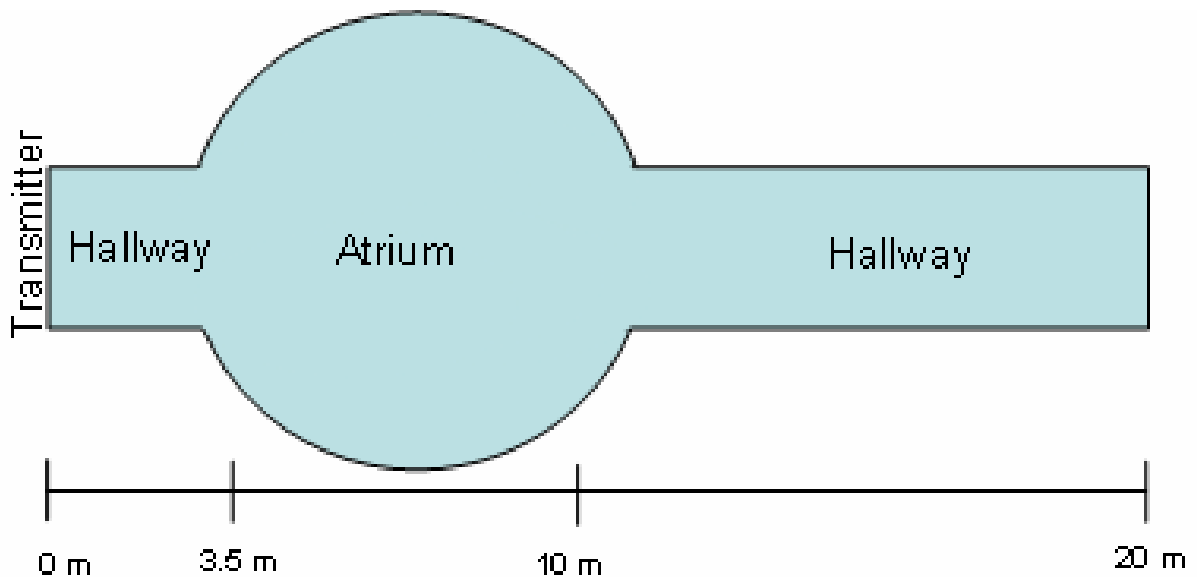


Figure 4-6. Floor layout of the atrium area in NEB.

The transmitter is held stationary at one end of the hallway, while the receiver and spectrum analyzer are moved away from the transmitter down the hallway, through the atrium and down into the extended hallway. The height above the floor of the transmitter and receiver factors into the amount of power received. Both the receiver and transmitter

are mounted approximately 0.5 meters above the floor. The transmitter is mounted onto the front end of a chair. The receiver is mounted onto a cart that also holds the spectrum analyzer and oscilloscope. Figure 4-7 shows the setup for the transmitter and the receiver.



Figure 4-7. Test setup.

Testing of a Self-Powered Wireless Sensor

After testing of the control system is complete, the control system is integrated with a sensor and reclaimed energy source to create a complete self-powered wireless sensor. Testing of the self-powered wireless sensor is more for verification purposes than detailed measurements. This testing provides proof that the control system works as it was intended as a portion of a self-powered wireless sensor.

Two versions of the self-powered wireless sensor are tested, one being powered from solar energy and the other powered from vibrations. The solar powered system uses a series of IXYS solar cells [33] and an energy harvesting circuit [34]. A flashlight is shined directly on the solar cells to provide a fixed light source. The vibration powered

system uses the bimorph PZT composite beams described earlier in this chapter. A Ling Dynamic Systems V408 shaker is used to vibrate the beams.

A hydrogen sensor with biasing circuit is used as the data input to the ADC of the control system. The biasing circuit receives its power from the same energy reclamation circuit as the control system. The hydrogen sensor is placed inside a custom built gas chamber as diagramed in Figure 4-8.

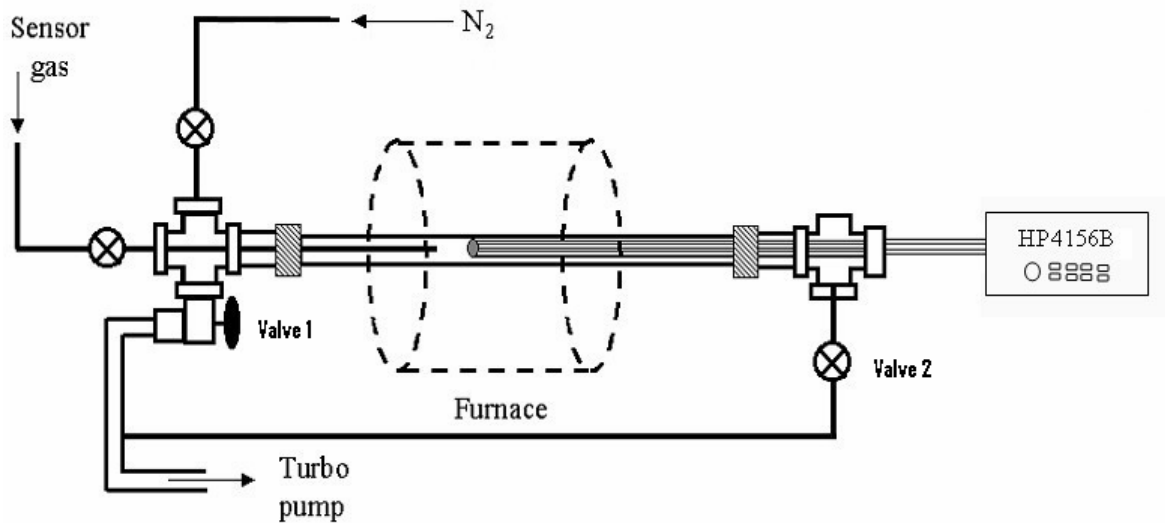


Figure 4-8. Gas chamber for testing hydrogen sensor.

The gas chamber consists of a glass tube with vacuum valves on both sides and a furnace surrounding the middle of the tube. The furnace was not operated for any of the experiments. Entering the gas chamber from the valve on the right is a hollow glass tube with wires running to a HP4156B Semiconductor Parameter Analyzer. The hydrogen sensor is placed inside this glass tube, and the wires from the parameter analyzer are connected to the hydrogen sensor in order to plot the IV characteristics of the sensor. Alternatively these same wires are used to connect the hydrogen sensor to the biasing circuit, which is placed outside of the gas chamber. A valve on the left side of the gas

chamber is connected to a gas cylinder containing 99.99% compressed nitrogen, a gas cylinder containing 500ppm of compressed hydrogen, and a turbo pump. The turbo pump is used to create a vacuum inside the gas chamber. A series of step by step procedures for setting up and operating the gas chamber to perform tests with the hydrogen sensor is described in the following paragraph.

Turn off the nitrogen and hydrogen gas lines and close both Valve 1 and 2. Open Valve 1 and wait for the pressure inside the chamber to drop below 0.01 torr (approximately 0 atm). Inside the gas chamber is now an approximate vacuum. Close Valve 1 and turn on the nitrogen gas line at maximum flow rate until the pressure inside the chamber reaches 760 torr (1 atm), then turn off the nitrogen gas line. The nitrogen is used to clear the gas chamber so that the hydrogen sensor starts from 0ppm of hydrogen. Turn on hydrogen gas line at maximum flow rate and open Valve 2. Opening Valve 2 connects the turbo pump, which creates a stream of 500ppm hydrogen gas flowing through the chamber and across the hydrogen sensor. The steps are repeated as many times as necessary to collect enough data and verify the different features of the self-powered wireless sensor.

CHAPTER 5 EXPERIMENTAL RESULTS

Characterization of the RF transmitter is presented in this chapter. Results of testing the ADC input of the microcontroller are given. The results of testing the control system including RF transmission tests, power consumption analysis, and functional verification are presented. This chapter also covers system integration test results for both the solar powered system and the vibration powered system.

RF Transmitter Characterization

The Ming TX-99 RF transmitter described in Chapter 3 was characterized using a Keithley 2400 Source Meter as a variable voltage supply for the V_{dd} supply input and a Tektronix CFG253 3MHz Function Generator for the data input. The function generator was set to output a 1 kHz square wave. The amplitude of the square wave was varied to determine the minimum data input level to successfully transmit the waveform to a Ming RE-99 RF receiver placed 1 foot away. The receiver was connected to a Tektronix TDS5104B digital phosphor oscilloscope to verify that the received signal matched the data signal from the function generator. The V_{dd} supply input was held constant at 9V, and the minimum data level was found to be 510mV. The next step was determining the minimum V_{dd} supply voltage to properly function with a 1V peak to peak data signal. The function generator was set to output a 1 kHz square wave that was 1V peak to peak with a 0.5V DC offset. The minimum V_{dd} supply voltage for this condition was 0.6V. To prove that the RF transmitter could operate using the on-off key technique, the signal

from the function generator was connected to both the data input and the V_{dd} supply input. The minimum peak to peak voltage of the function generator was found to be 530mV in order to get the correct signal at the receiver.

Since the transmitter will be operated at 2V from the microcontroller output, further testing was done to determine the transmission power. A SMA connector was soldered to the antenna output of the TX-99 transmitter. An Agilent E3631A DC power supply was connected to the V_{dd} and data inputs on the TX-99. A FLX402#1 1 foot SMA cable was used to attach the SMA connector on the TX-99 to a DC blocker on the input of a Hewlett Packard 8563E spectrum analyzer. The spectrum analyzer measured a transmit power of -4.5dBm from the TX-99. Figure 5-1 shows the screen capture from the spectrum analyzer.

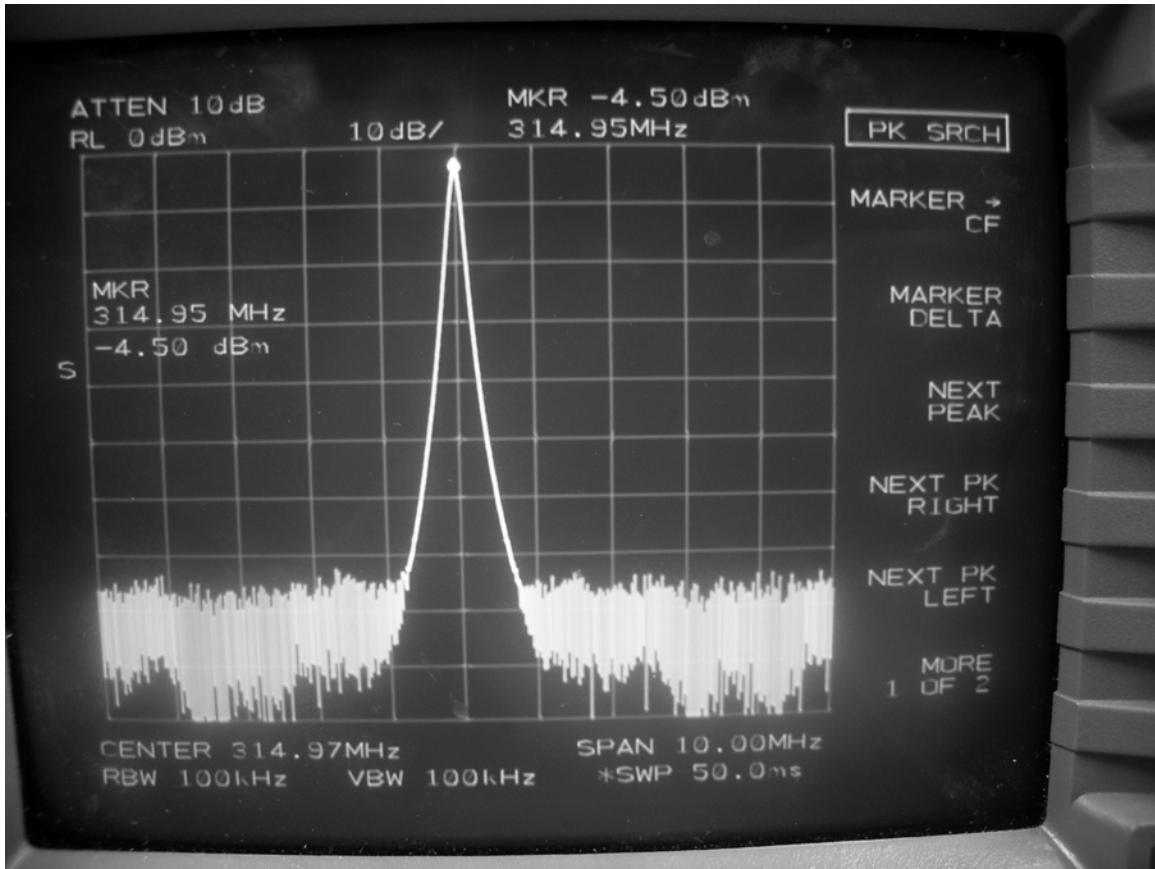


Figure 5-1. Transmit power from Ming TX-99 RF transmitter.

ADC Testing

Various devices were used to verify the operation of the ADC of the microcontroller. The microcontroller was programmed to simply take the input from the ADC, encode the analog input to a 10 bit value, and then serially shifted the 10 bits out onto an output pin. The output pin was connected to a Tektronix TDS5104B digital phosphor oscilloscope to verify that the output data matched the data input to the ADC. Initially the ADC was connected to a Keithley 2400 Source Meter which was set to output a fixed voltage so that the encoded data would be easy to decode when viewed on the oscilloscope. The data on the scope was a 10 bit serial stream that represented an encoded value based on a percentage of the microcontroller's supply voltage. The

microcontroller's supply voltage was connected to a Tektronix PS281 DC Power Supply which was set to output 2V. The ADC input was varied from 0V to 2V and the bit stream on the scope was visually verified to coincide with the value of the input on the ADC.

Testing of the Control System

Testing the control system consists of testing the microcontroller connected to the RF transmitter to determine the RF transmission characteristics, power consumption, and to verify the functionality of the system. The microcontroller was programmed with the data transmitting code. Due to the need for a sampled voltage on the ADC input a fixed voltage supply was required in order to control the value of the transmitted data. The power consumption was analyzed over the entire code routine, from initialization through an entire cycle of reading the ADC and transmitting data. Delays in the code were modified to make it easier to separate each step of the code. The functionality of the system was verified using both the level monitoring code and the data transmitting code.

RF Transmission

The RF transmitter was connected to the microcontroller and experiments were done in order to determine the maximum transmission distance, the received power, and the frequency spectrum of the received signal. For all experiments the microcontroller's supply voltage was connected to a Keithley 2400 Source Meter set to 2V. The microcontroller's ADC was connected to another Keithley 2400 Source Meter so that the transmitted signal could be controlled. An Agilent E4448A PSA series spectrum analyzer was used to measure the frequency spectrum and the received power. Figure 5-2 and Figure 5-3 show the received power and spectrum at 300 MHz for distances of 1 meter and 8 meters with a $\frac{1}{4}$ wave whip antenna connected to the transmitter's antenna connector. At distances above 8 meters, the received power was barely above the noise

floor of the spectrum analyzer. Figure 5-4 plots the received power measured from the spectrum analyzer for various distances. The bounce back in the slope of the plot at 10 meters is attributed to a wave guide caused by the shape of the room where testing took place.

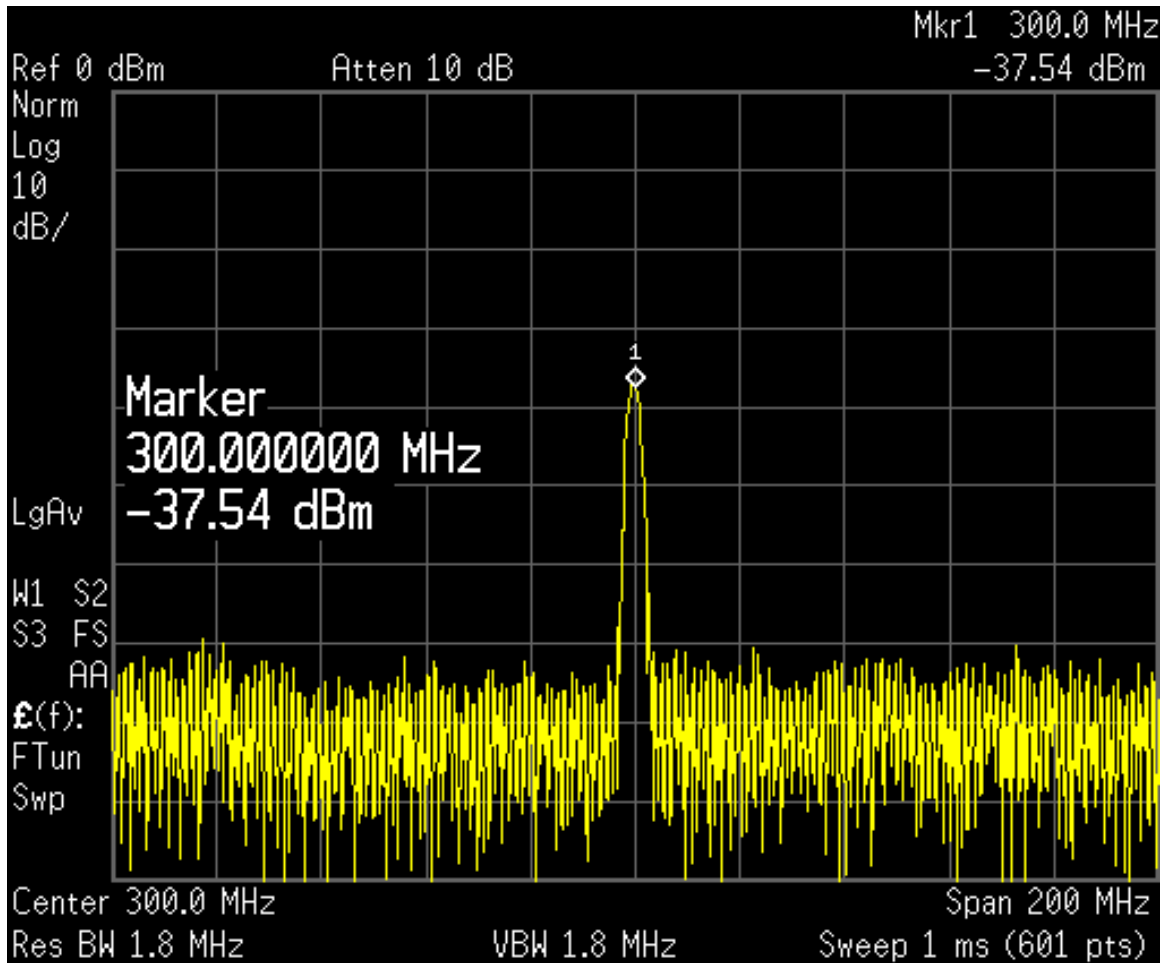


Figure 5-2. Received spectrum at 1 meter from transmitter.

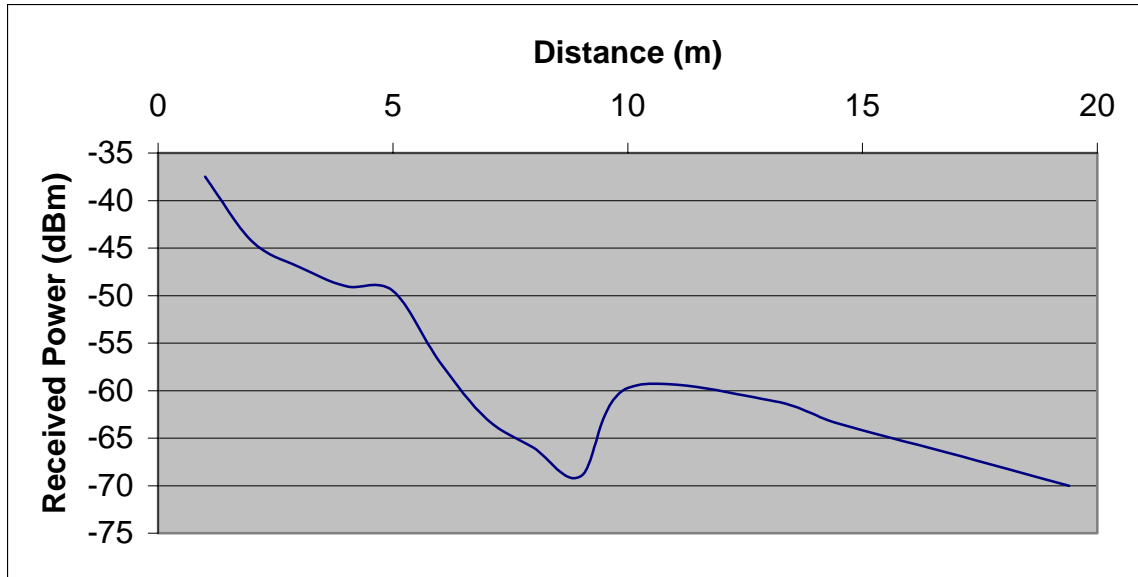


Figure 5-4. Received power at varying distance from transmitter.

The Ming RE-99 receiver was connected to a Tektronix TDS210 two channel digital real-time oscilloscope to verify that the data received matched the data transmitted. Above 8 meters the received signal started to deteriorate. To illustrate the deterioration Figure 5-5 shows the received signal at 8 meters and Figure 5-6 shows the received signal at 10 meters. Tests were continued until the received signal no longer looked like the transmitted signal. Figure 5-7 shows the received signal at 14.5 meters. Antennas were used on the transmitter and receiver to attain an even greater transmission distance. Table 5-1 lists the maximum transmission distances for the different antenna locations.

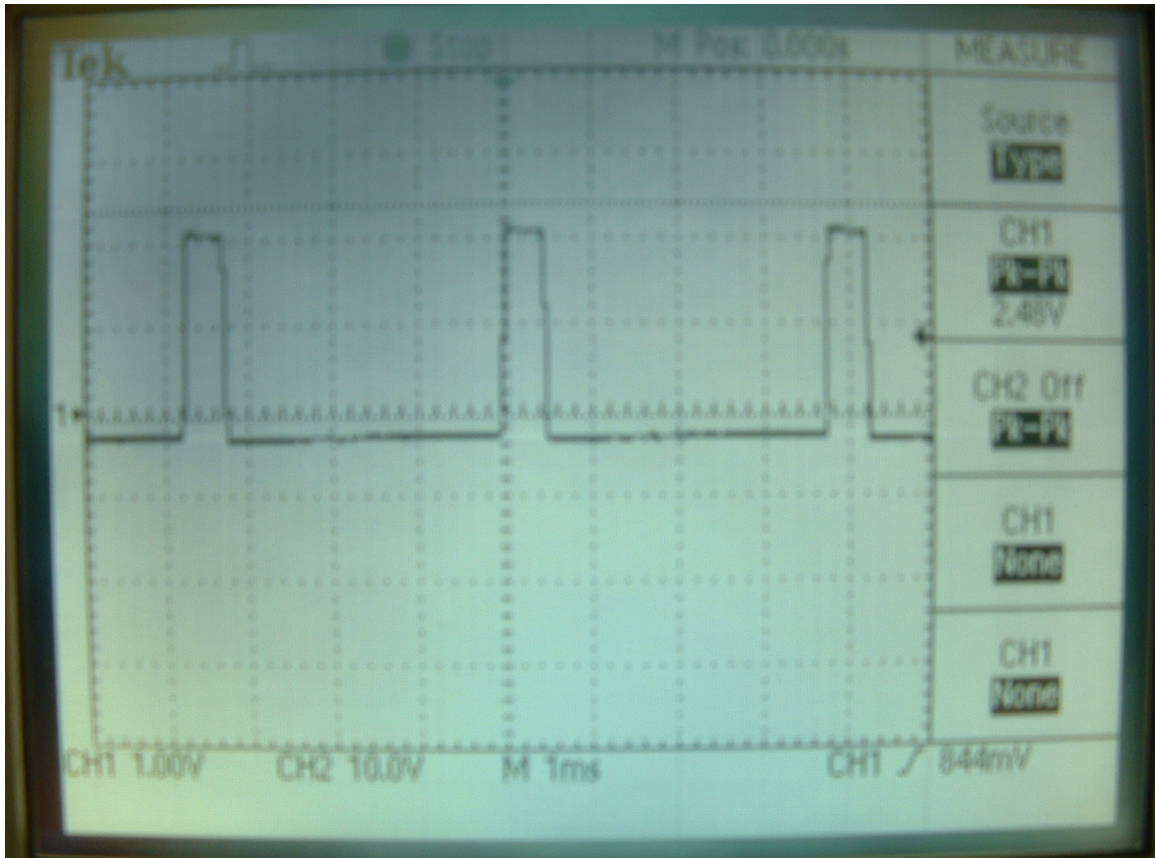


Figure 5-5. Received signal at 8 meters.

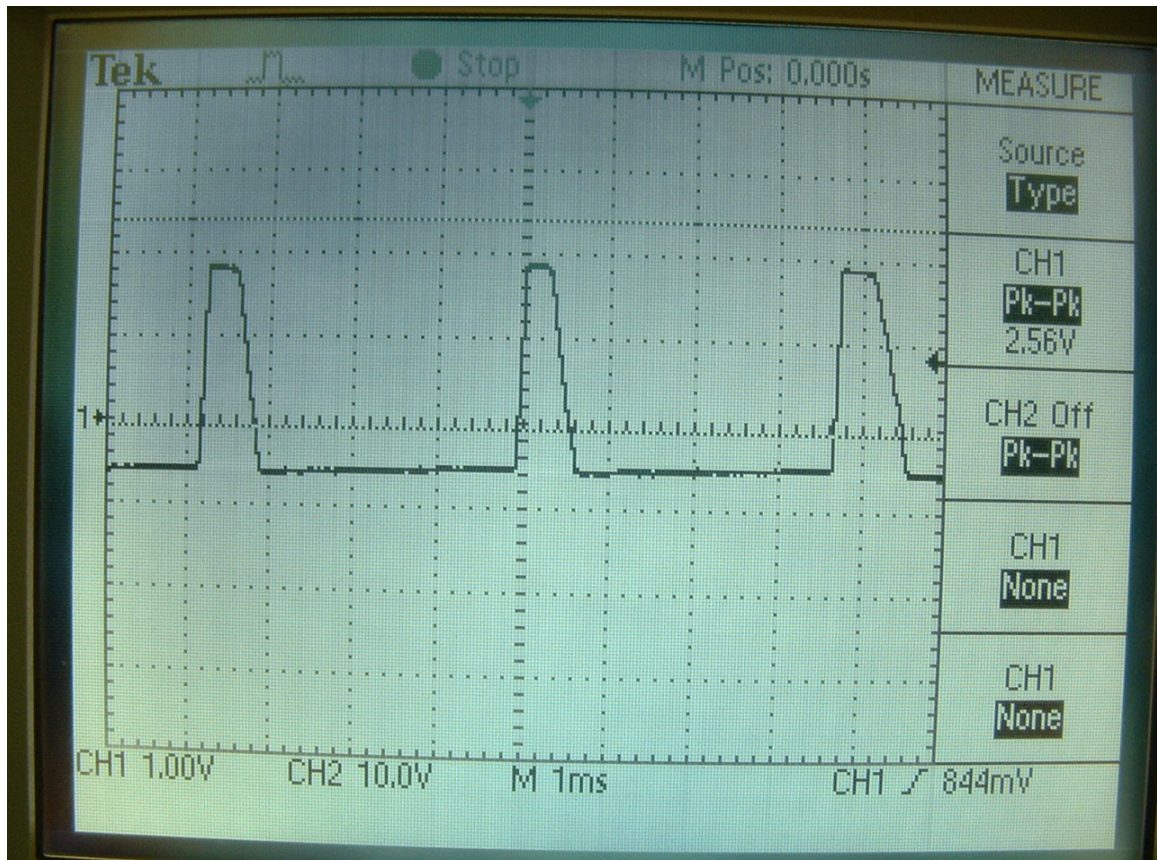


Figure 5-6. Received signal at 10 meters.

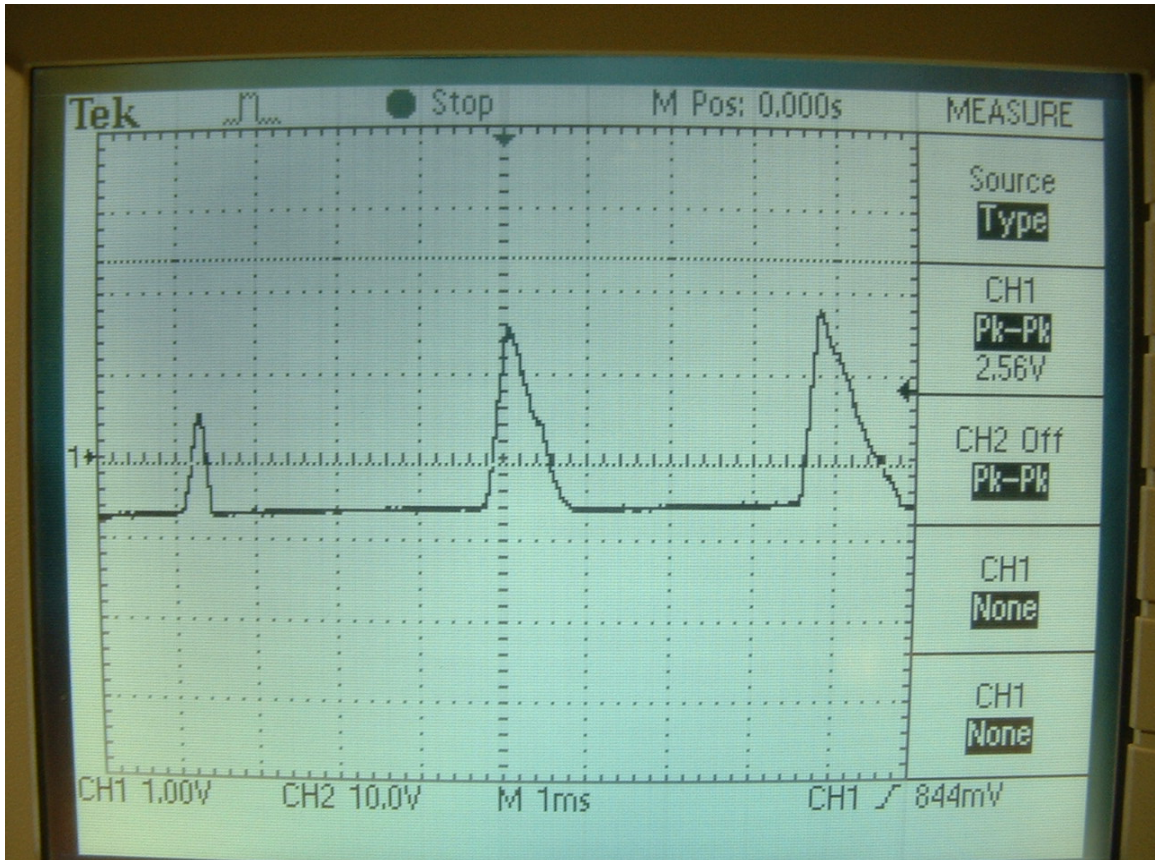


Figure 5-7. Received signal at 14.5 meters.

Table 5-1. Maximum transmission distances for different antenna locations.

Antenna Locations	Maximum Distance
Receiver Only	14.5 m
Transmitter Only	16.8 m
Transmitter & Receiver	19.4 m

Power Consumption

The power consumption of the control system is broken down into the power consumed during different activities of the system. The power was measured for initialization, sensing data, transmitting data and remaining idle. Both modes of operation require the same initialization code, therefore the initialization power is the

same. Figure 5-8 shows a scope capture of the voltage measured across the 383 Ohm resistor during initialization. Since the resistor is constant and the supply voltage is a constant 2V, initialization power has the same shape as the voltage across the resistor. The value of the initialization power at any point along the scope capture is calculated using the equation

$$P_{\text{init}} = 2V * V_{\text{meas}} / 383 \text{ Ohms}, \quad (5-1)$$

where V_{meas} is the voltage measured in the scope capture. From the scope capture the duration of the initialization phase was found to be 12.5 ms. The peak power during initialization was 7.3 mW. The average power during initialization was found by separating the scope capture into linear segments and calculating the area under each segment then summing the areas together and multiplying the resulting sum by the total time duration for initialization. The average power during initialization was calculated to be 3.07 mW. The energy required for initialization is simply the total initialization time multiplied by the average power during initialization. The initialization energy was calculated to be 38.4 μJ .

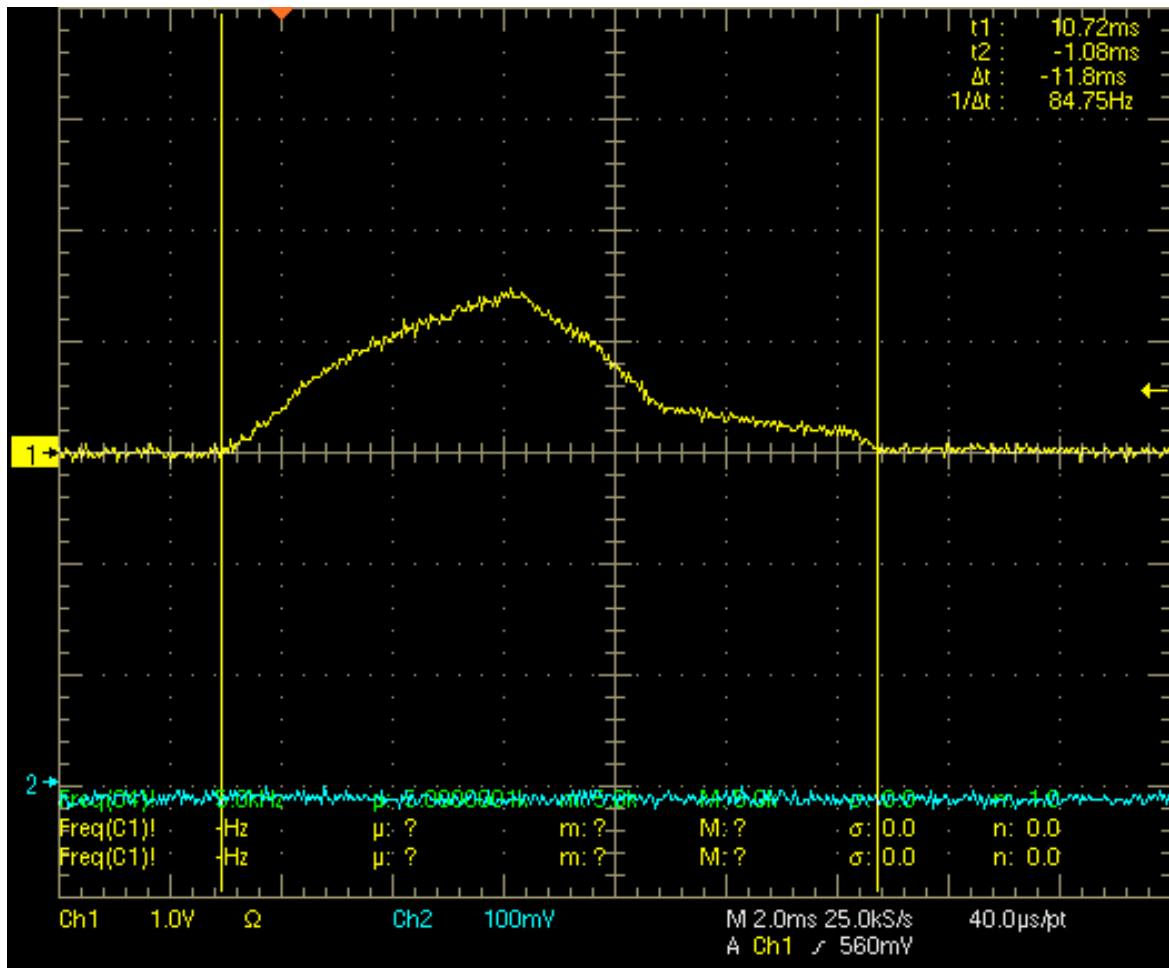


Figure 5-8. Scope capture of voltage across series resistor during initialization.

The code was written using sleep modes, so that the ADC sampling does not require any additional power compared to remaining idle. Therefore the power during the idle state and power during the ADC sample state are the same. Figure 5-9 shows a scope capture of the voltage measured across the 383 Ohm resistor during an idle state. Since the voltage is in the noise range of the scope and is less than 50 mV, the average power was found by using a Keithley 2400 Source Meter which has a feature that displays the output supply current and supply power. The displayed average output power was 2.5 μ W.

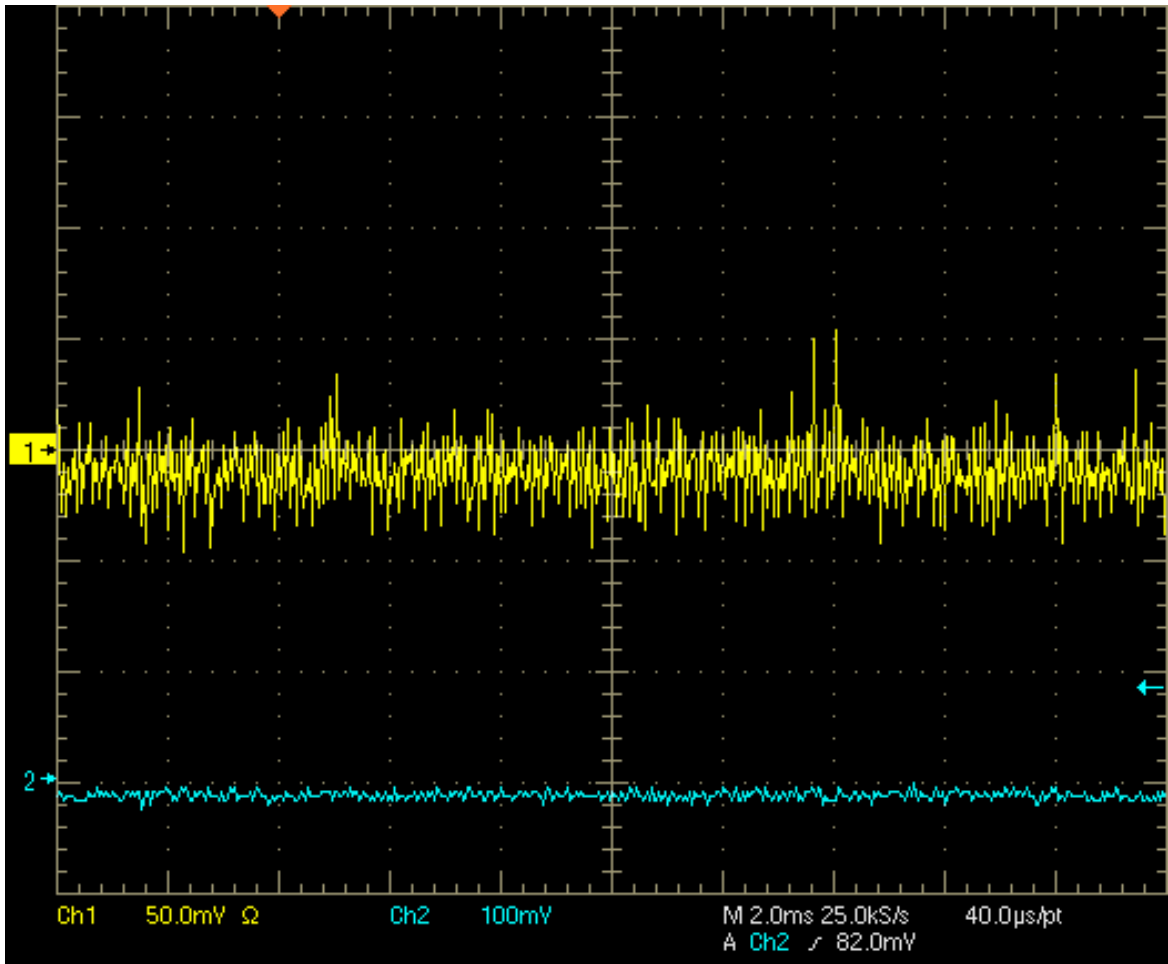


Figure 5-9. Scope capture of voltage across series resistor during idle state.

The amount of power required to transmit data was measured for various transmission cases. Since the RF transmitter is operating in an on-off key mode, the amount of power required to transmit data is directly related to the data being transmitted. With on-off keying there is no additional power, above the power required to remain idle, to transmit a “0” valued bit. Additional power is only required when transmitting a “1” valued bit. For the case of level detection, the power required is simply the power required to send a single “1” valued bit of data. Figure 5-10 shows a scope capture of the power required to transmit a single “1” valued bit of data, as well as the single bit of data being transmitted. Figure 5-11 shows a zoomed in view of the same scope capture as

Figure 5-10, focusing on the rise time of the transmit power. While the rise time is equal to the same amount of time the transmitted bit is sent, the remaining 5.5 ms of fall time is due to the slow discharge of the LC circuit in the RF transmitter. The average power to transmit a single “1” valued bit was calculated similarly to the initialization power. The calculated value for average power to transmit a single “1” valued bit was $303 \mu\text{W}$. Since the total time for transmit power is 6 ms, the average energy required to transmit a single “1” valued bit of data is $1.8 \mu\text{J}$. In Figure 5-11, an apparent overlaying frequency exists on the scope capture of the power. This switching frequency is due to the oscillation of the LC circuit in the RF transmitter which is used to generate the transmitted signal’s frequency.

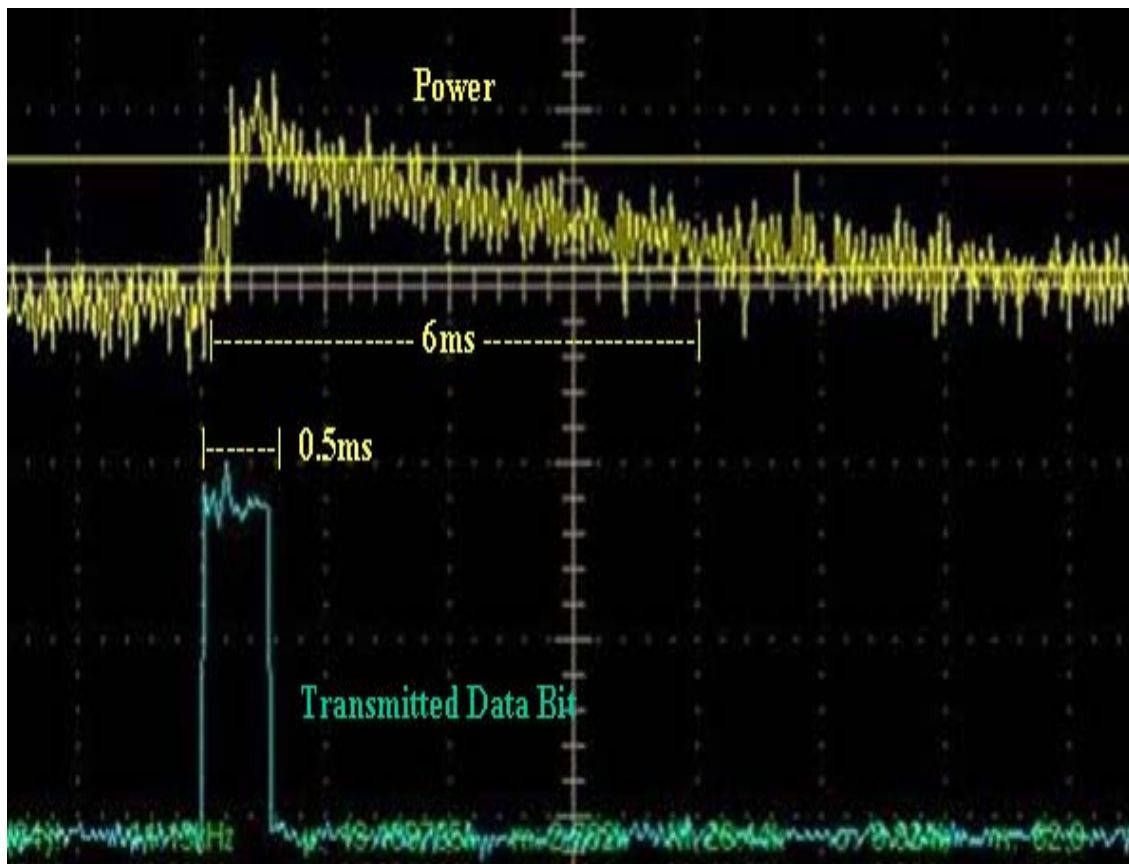


Figure 5-10. Transmit power for a single data bit.

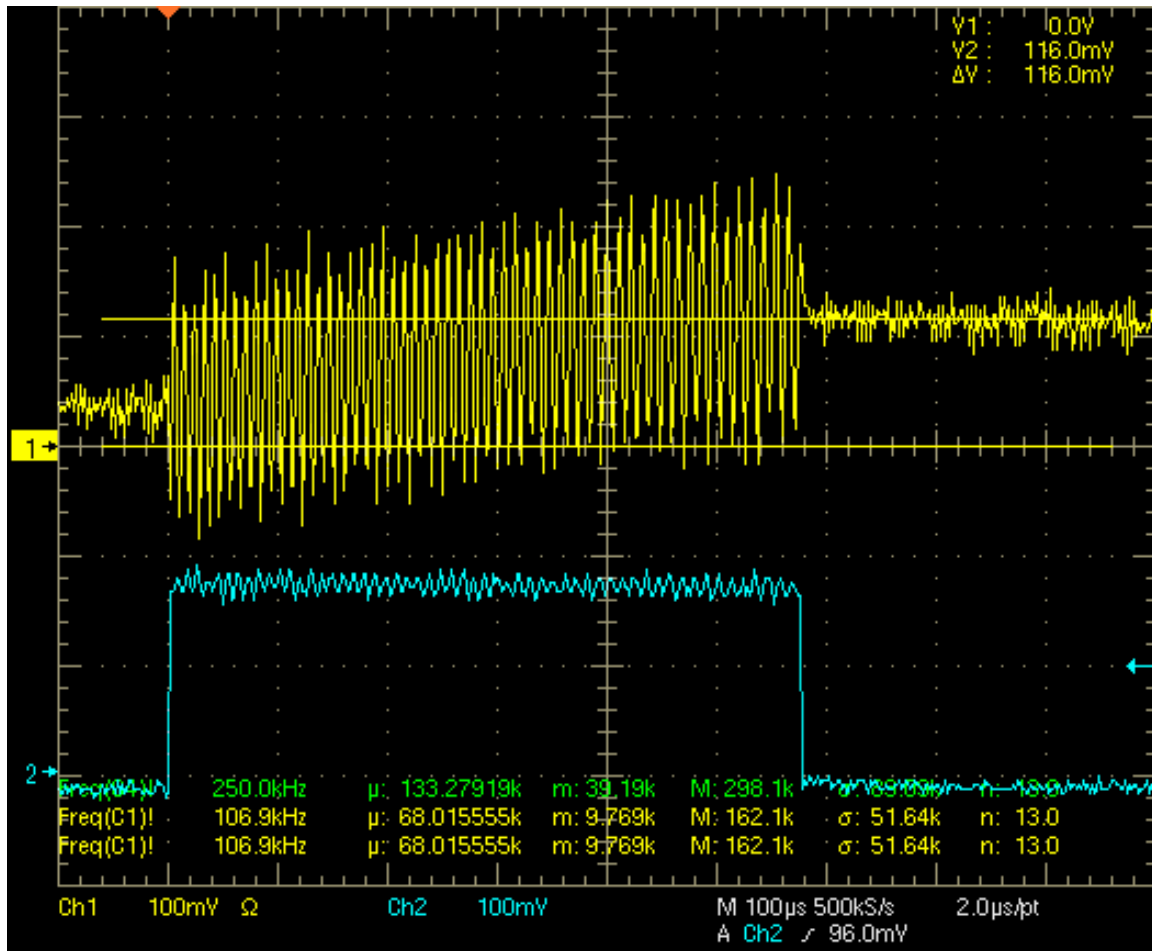


Figure 5-11. Zoomed in view of transmit power for a single data bit.

Measurements were taken during transmission of mixed data patterns. Scope captures of the power along with the data pattern are shown in Figure 5-12, Figure 5-13, and Figure 5-14. The slope of each rising and falling segment of the transmit power is the same as the rising slope and falling slope of the transmit power for a single “1” valued bit. The rising slope represents the power during a “1” valued bit. The falling slope represents the power during a “0” valued bit. The length of time for each segment of rising and falling slope is based on the number of consecutive “1” valued bits or “0” valued bits. The scope captures clearly show that the power is dependant on the bit order, with every “0” valued bit transmitted after a “1” valued bit decreasing the total power.

Therefore, the maximum power would occur when all the “1” valued bits were transmitted in a row. This can clearly be seen in Figure 5-15, which shows 3 different bit patterns all with the two “1” valued bits for six transmitted bits. Note that the area under the waveform after the sixth bit will always be the same for any given number of “1” valued bits. The area under the waveform is greatest when all the “1” valued bits are transmitted one after the other. Thus the maximum energy used occurs when all “1” valued bits are transmitted one after the other. Using the waveform that represents the maximum energy will allow for a simplification in determining the maximum average power, for any given number of “1” valued bits per transmission. The peak of the triangular pulse is simply the peak value for transmitting a single “1” valued bit times the total number of “1” valued bits transmitted. Since the waveform has a triangular shape, the area under the waveform which represents the maximum energy required is equal to $\frac{1}{2}$ the peak power times the total time. The maximum average power required to transmit any given data pattern can be calculated simply by multiplying the average power to transmit a single “1” valued bit by the number of “1” valued bits transmitted. The maximum average power during transmission is calculated using the equation

$$P_{tx} = N_1 * P_1, \quad (5-2)$$

where N_1 is the number of “1” valued bits, and P_1 is the average power to send a single “1” valued bit. Figure 5-16 lists the maximum average power during transmission for various number of “1” valued bits transmitted.

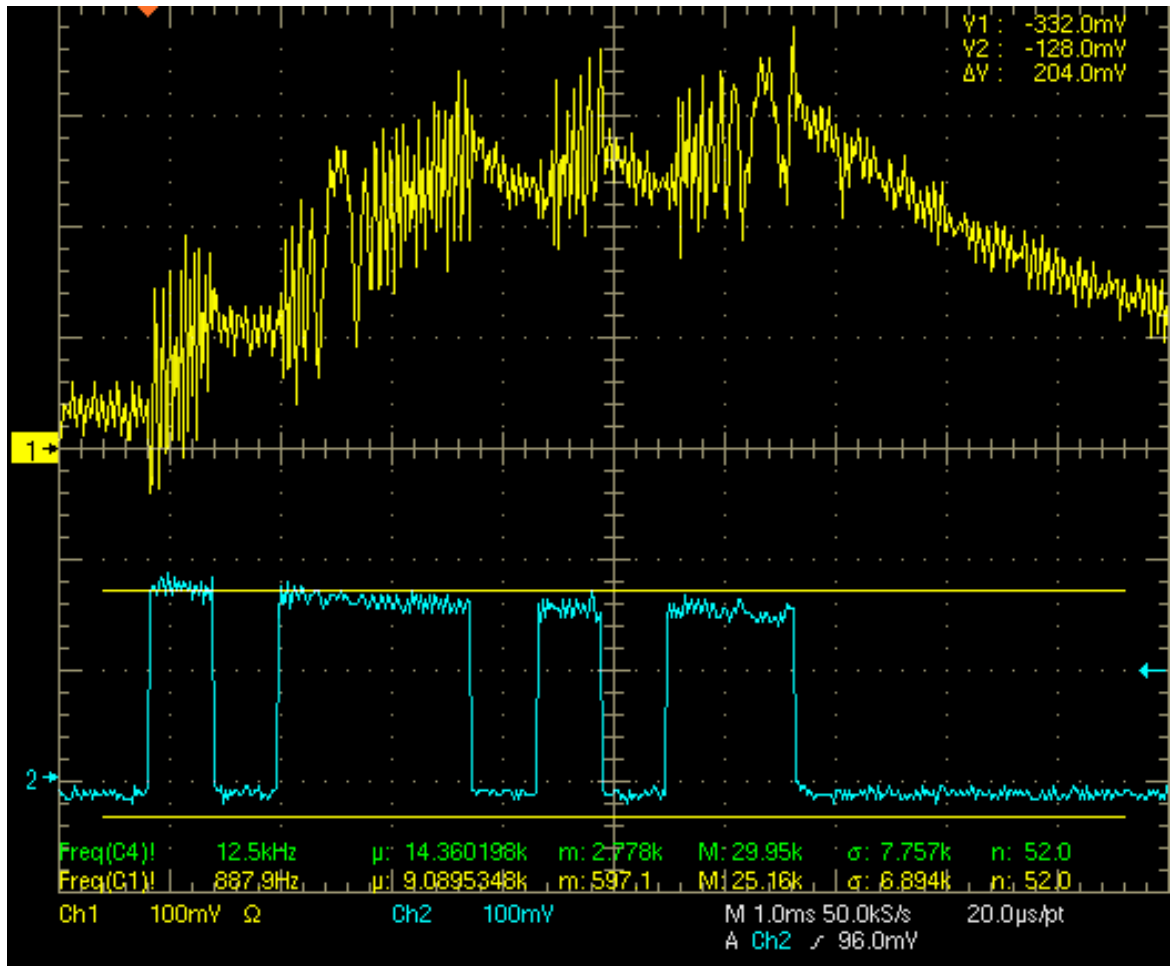


Figure 5-12. Scope capture of transmission power for data pattern '1011101011'.

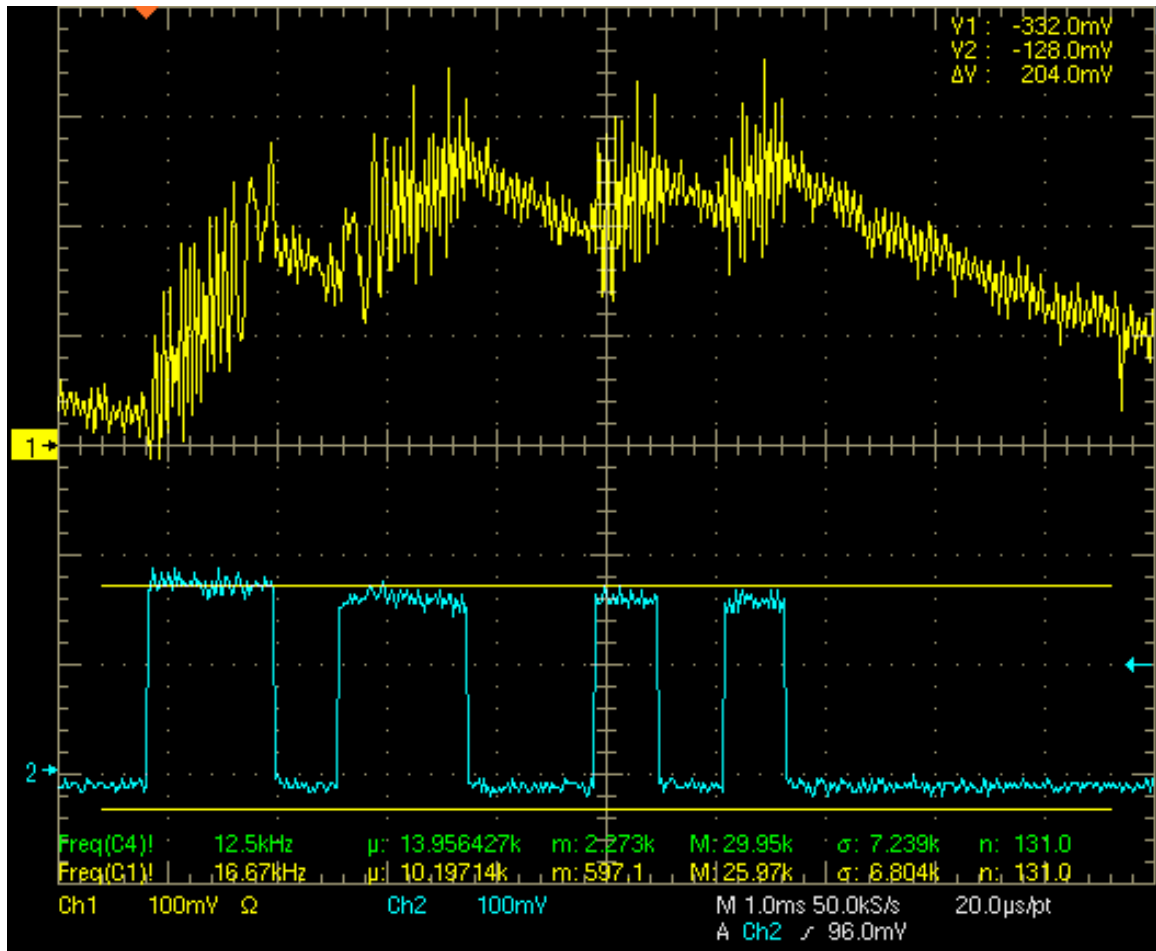


Figure 5-13. Scope capture of transmission power for data pattern '1101100101'.

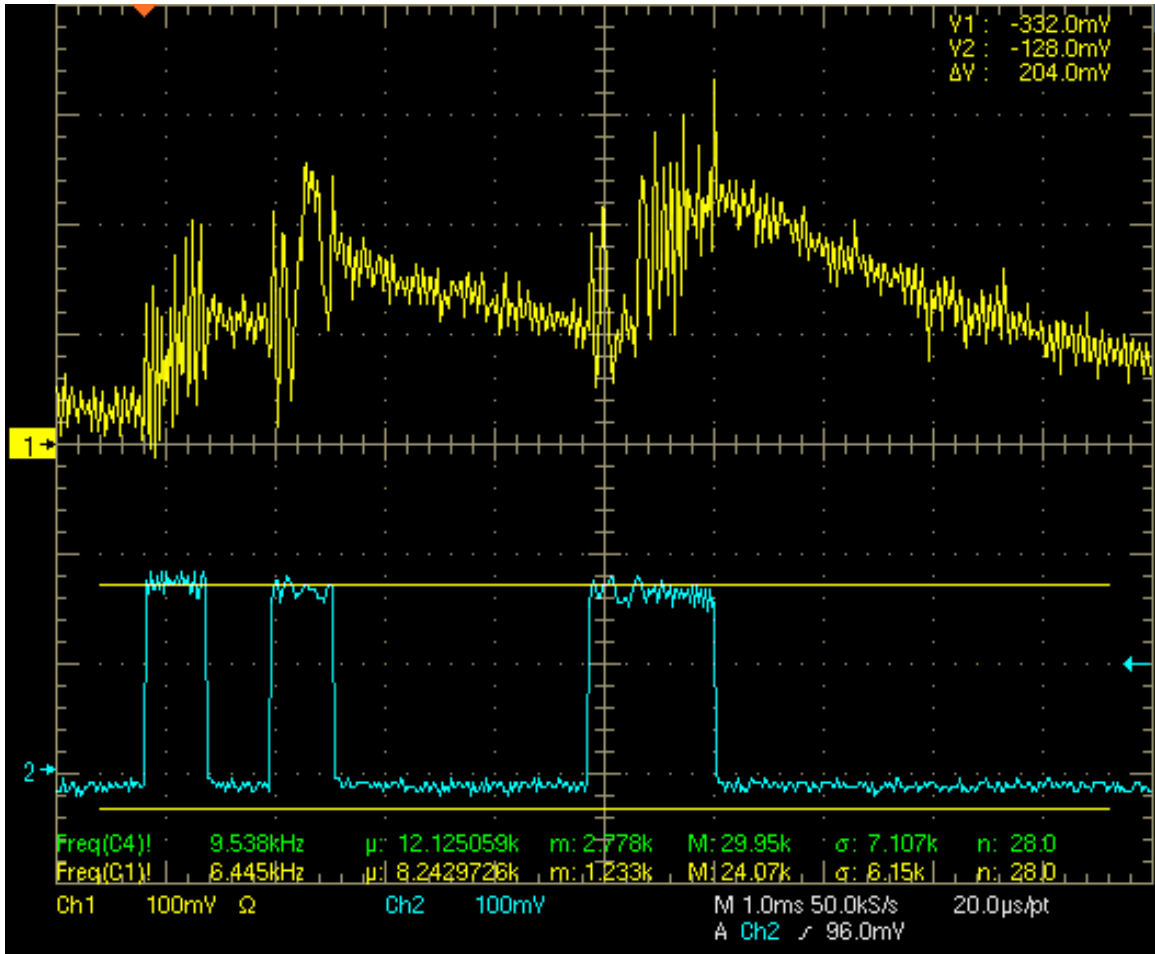


Figure 5-14. Scope capture of transmission power for data pattern '1010000110'.

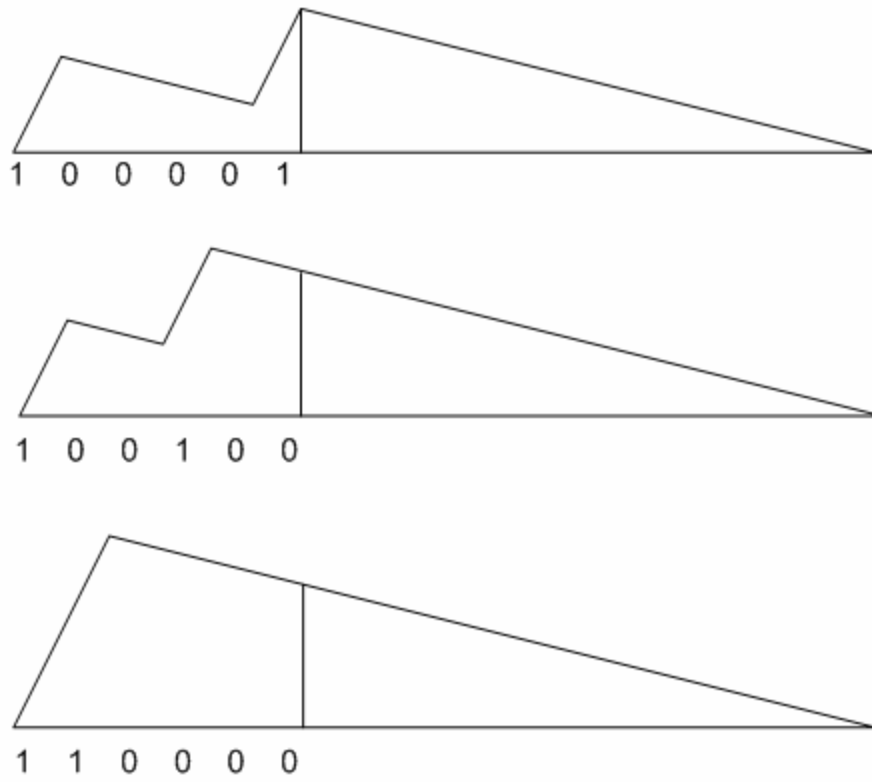


Figure 5-15. Different data patterns for two "1" valued bits.

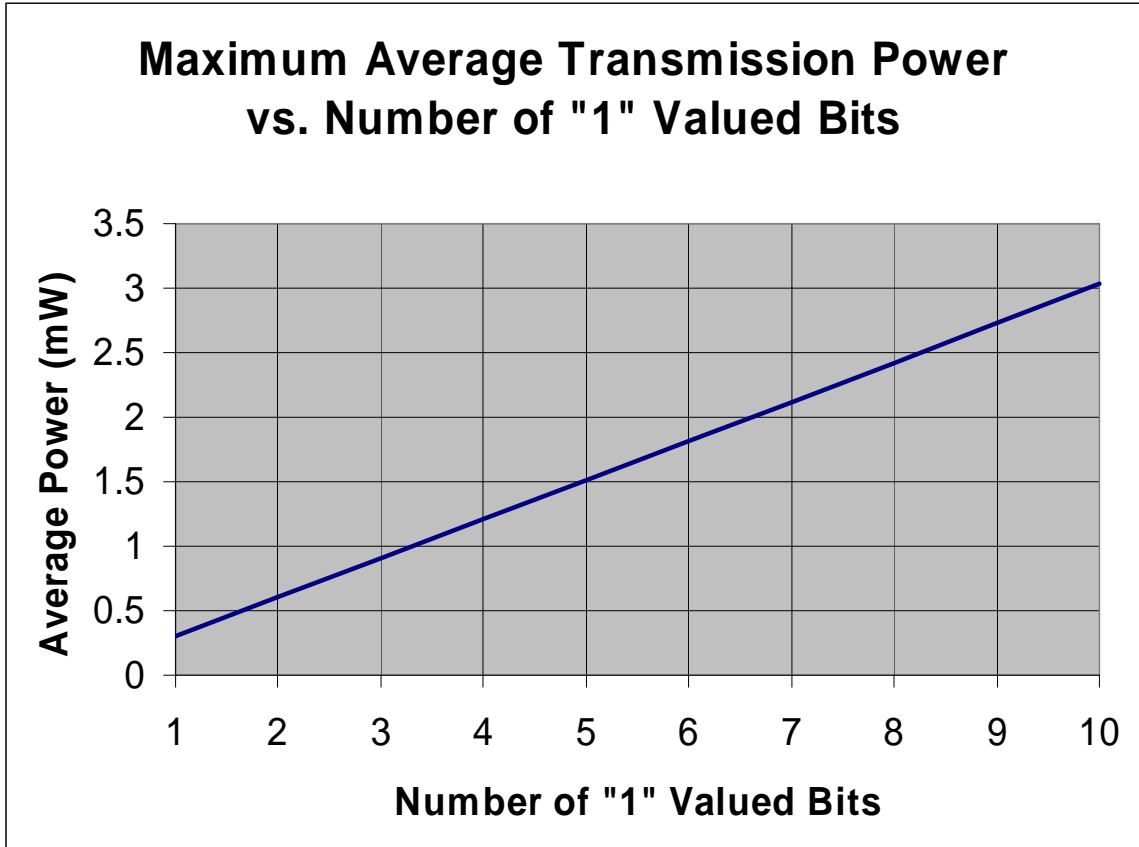


Figure 5-16. Maximum average transmission power vs. number of "1" valued bits.

The average power across an entire cycle of sampling and transmitting data is dependant on the delay times set in the code as well as the number of "1" valued bits being transmitted. The following equation is used to determine the average power for an entire sample and transmit cycle.

$$P_{\text{cycle}} = (P_{\text{ADC}} * t_{\text{ADC}} + P_{\text{idle}} * t_{\text{idle}} + P_{\text{tx}} * t_{\text{tx}}) / t_{\text{total}} \quad (5-3)$$

Where P_{ADC} is the average power during ADC sampling, t_{ADC} is the amount of time to perform an ADC sample, P_{idle} is the average power idling, t_{idle} is the amount of time in an idle state, P_{tx} is the average power during transmission, t_{tx} is the amount of time to perform a transmission, and t_{total} is the total amount of time to perform an entire cycle.

Since the average power during ADC sampling is the same as the average power for remaining idle, Equation 5-3 can be simplified to the following equation.

$$P_{\text{cycle}} = (P_{\text{no_tx}} * t_{\text{no_tx}} + P_{\text{tx}} * t_{\text{tx}}) / t_{\text{total}} \quad (5-4)$$

Where $P_{\text{no_tx}}$ is the average power during ADC sampling and idling or in other words when not transmitting, $t_{\text{no_tx}}$ is the amount of time during the cycle when not transmitting data. The total time for a cycle is equal to the time when transmitting plus the time when not transmitting (i.e. $t_{\text{total}} = t_{\text{tx}} + t_{\text{no_tx}}$). The time parameters can be re-written in terms of duty cycle. The duty cycle for transmitting data compared to the rest of the cycle time is defined as

$$D_{\text{tx}} = t_{\text{tx}} / t_{\text{total}}. \quad (5-5)$$

Substituting the duty cycle into Equation 5-4 yields the following equation,

$$P_{\text{cycle}} = [P_{\text{no_tx}} * (1 - D_{\text{tx}})] + (P_{\text{tx}} * D_{\text{tx}}) \quad (5-6)$$

which is completely a function of the average powers and transmission duty cycle.

Ultimately, this equation can be rewritten using Equation 5-2 so that the only dependencies are the number of “1” valued bits and the duty cycle. The resulting equation for average power during a complete cycle is

$$P_{\text{cycle}} = [2.5\mu\text{W} * (1 - D_{\text{tx}})] + (303\mu\text{W} * N_1 * D_{\text{tx}}) \quad (5-7)$$

In the case of level monitoring only one “1” valued bit is transmitted. The transmission duty cycle versus the average power for the case of level monitoring versus is shown in Figure 5-17. The power to remain idle dominates the average power up to a duty cycle of 0.1%. At 1% duty cycle the average power is twice the idling power, and the average power continues exponentially from there before topping off at 303 μW for a case when the system is constantly transmitting.

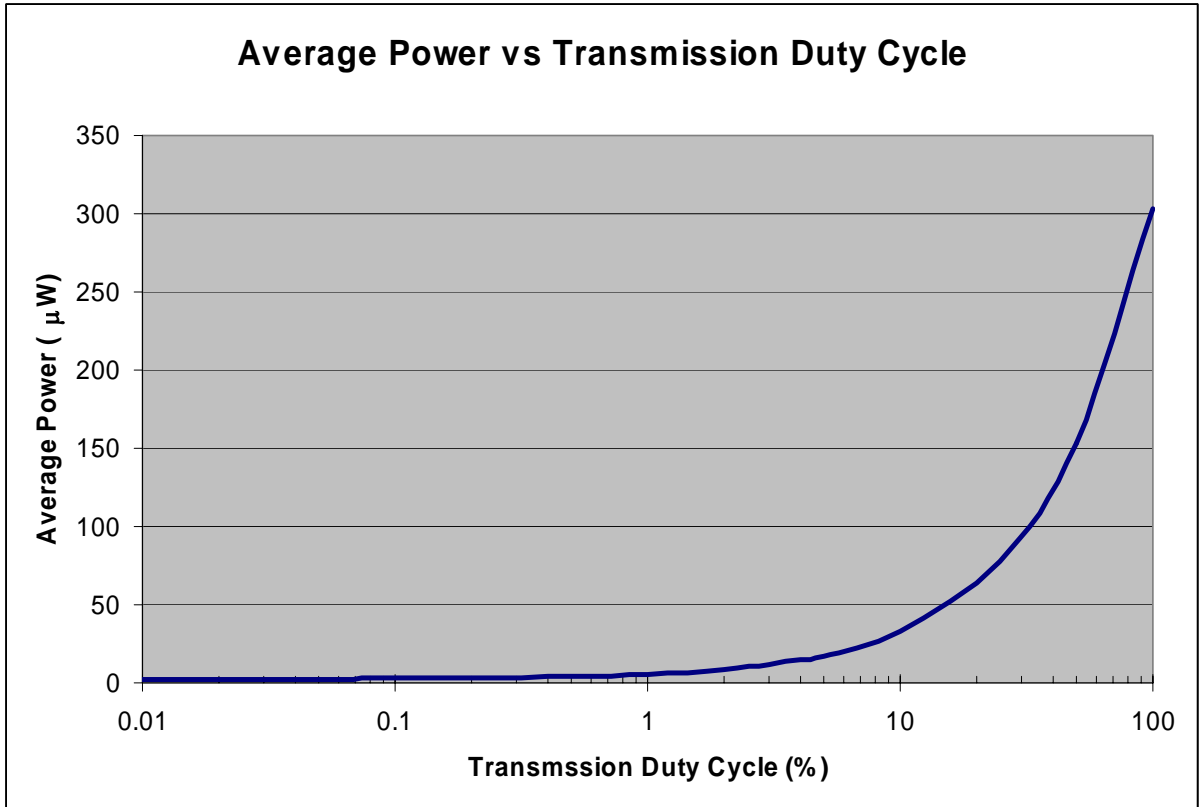


Figure 5-17. Duty cycle vs. average power for level monitoring.

Functional Verification

By performing the transmission tests the functionality of the control system was tested. Both the level monitoring and data transmitting versions of code were verified to work properly. A Keithley 2400 Source Meter was used to control the input to the ADC. The RE-99 receiver was connected to a Tektronix TDS210 two channel digital real-time oscilloscope, to monitor the received signal.

For the case of level monitoring, the source meter was set below the trigger level and no data was seen on the oscilloscope. Once the source meter was set above the trigger level a single bit was visually verified on oscilloscope. The source meter was set back below the trigger level and then the experiment was repeated and a single bit was again seen on the oscilloscope.

For the case of data transmitting, the source meter was set to 0 V and no data was seen on the oscilloscope. The source meter was then set to 2 V and a single 5 ms long pulse was seen on the oscilloscope. The source meter was varied from 0 V to 2 V, and varying data patterns were seen on the oscilloscope.

System Integration

The complete self-powered wireless sensor tested consisted of the control system, the hydrogen sensor, and an energy harvesting circuit. The control system was operated in level monitoring and data transmitting modes. The hydrogen sensor required a biasing circuit as described in Chapter 4. Two different energy harvesting circuits were used, one for solar energy and the other for energy from vibrations. In both cases enough power was generated to operate the control system as well as to provide the power to bias the hydrogen sensor.

The level monitoring code was edited so that 100 ppm hydrogen would trigger the transmission of an emergency pulse. With no hydrogen present in the gas chamber the level monitoring mode never transmitted any emergency pulses. Once hydrogen was introduced into the gas chamber within a few minutes an emergency pulse was transmitted.

The data monitoring code was run with no hydrogen in the gas chamber and an all 0's valued transmission was received by the RE-99 receiver and displayed on a Tektronics TDS224 Four Channel Real Time Oscilloscope. Once hydrogen was introduced into the gas chamber the received signal started to vary, with the encoded value increasing over time. After a longer period of time the hydrogen sensor reached a steady state value as became apparent when the received data remained constant. Once

steady state was reached the hydrogen was flushed from the gas chamber and the received data started to vary again until finally settling back at a value of all 0's.

CHAPTER 6 CONCLUSIONS

The control system designed in this thesis has conclusively been proven to work. This chapter summarized the work presented in this thesis. Conclusions drawn from the work as well as potential future work are also discussed in this chapter.

Conclusions

An ultra-low power control system for a self-powered wireless sensor has been designed, tested and its functionality has been verified. The control system has been optimized for minimal power consumption, based on the results of testing the sections of the design. The average power has been measured for all portions of the design, and has been minimized in accordance with the test results. Equations have been generated to calculate the average power required based on the number of transmitted bits and the duty cycle of transmission. The RF transmission has been characterized based on the series of measurements described in this thesis.

The average power was ultimately defined as a simple equation with the two variables being the duty cycle of transmission, and the number of 1's valued bits being transmitted. However, regardless of the value of the data being transmitted the frequency that data is transmitted is the main factor in determining the average power. For a transmission duty cycle of less than 0.1% the transmit power barely factors into the total and the average power is dominated by the idle power which is $2.5 \mu\text{W}$.

The transmitter was not optimized other than operating it using on-off keying. The maximum transmission distance with antennas was measured to be 19.4m. Due to

constraints on the area available for the RF transmission, the maximum transmission distance may vary from the measurements. However this thesis was not focused on the transmission characteristics, but rather the design of an operational system.

The control system was designed to be very flexible so that future designs could easily modify the microcontroller code to adapt to a specific application. The microcontroller code was designed to minimize the power required by holding the microcontroller in a sleep mode once the initialization sequence is complete. Two separate sets of code were written to minimize the processing time for a system that requires transmission only when a sensor's data is above a given value versus a system that requires data transmission at a given interval. However simple adjustments in the code could easily be written to make a single system that does both fixed interval transmission as well as emergency pulse transmissions if the sensor's data reaches a given value.

Future Work

The control system was designed for ultra low power however the transmitted power can be minimized by encoding the data in order to minimize the number of bits transmitted. Further development can be done to minimize the power required by the RF transmitter. The RF transmitter should be designed for the exact application and deployment of the system. Using an antenna chamber a more accurate characterization of the RF signal could be attained.

More work can also be done on the energy harvesting circuits so that a variety of energy sources can be used simultaneously, thus minimizing the reliance on a single source of energy. The energy harvesting circuits can also be made more efficient so that less total energy is required into the complete system. Similarly more efficient solar cells

and PZT beams would enable operation in systems with lower levels of available energy. Less required energy would translate to smaller sized solar cells or PZT beams, and hence a smaller total package size of the system which would allow deployment of the system in more applications.

This system could be used as a single node in a multi-node array of wireless sensors. However some form of protocol would have to be defined for the transmitted data in order to operate several of these sensors within a given area. Additionally, a multi-node array would require a more advanced receiver than the RE-99 used for this design.

APPENDIX MICROCONTROLLER PROGRAM CODE

The program code for the microcontroller is included here. Two versions of code are given, one for level monitoring and the other for data transmitting.

Code for Level Monitoring

```

//*****
//
// Description: Level Monitoring
//
//           MSP430F1232
//           -----
//           /\ |           XIN|-----\
//           | |           | Crystal
//           |--|RST      XOUT|-----^
//           |           |
//           |           P1.0|--> RF Transmitter
// sensor-->|ADC         |
//           -----
//
// David Johnson
// University of Florida
// August 2005
//*****

#include <msp430x12x2.h>

void main(void)
{
    WDTCTL = WDTPW + WDTHOLD;           // Stop WDT
    P3DIR |= 0x10;                       // Set P1.0 to output direction
    P3OUT = 0x00;                         // Set the output to 0x0
    ADC10CTL0 = ADC10SHT_2 + ADC10ON + ADC10IE;
    CCTL0 = CCIE;                         // CCR0 interrupt enabled
    CCR0 = 500;                           // Delay for Sampling
}

```

```

TACTL = TASSEL_1 + MC_1;           // ACLK, upmode

__EINT();                          // Enable interrupts.
ADC10AE |= 0x01;                   // P2.0 ADC option select
LPM3;

}

// ADC10 interrupt service routine
#pragma vector=ADC10_VECTOR
__interrupt void ADC10_ISR (void)
{
    static int output_already;      // Variable to determine if Transmitted to Output
    if (ADC10MEM < 0x1FF)
    {
        P3OUT = 0x00;              // Set output LOW
        output_already = 0;        // Reset variable
    }

    else if (output_already == 0)
    {
        output_already = 1;        // Set variable so transmission only occurs once
        P3OUT = 0x10;              // Set output HIGH
        int pulse_length;
        for (pulse_length = 100; pulse_length>0; pulse_length--); // Wait with output HIGH
        P3OUT = 0x00;              // Set the output LOW
    }

    else                            // Occurs if threshold has already been reached
    {
        output_already = 1;        // Holds variable
    }
}

// Timer A0 interrupt service routine
#pragma vector=TIMERA0_VECTOR
__interrupt void Timer_A (void)
{
    ADC10CTL0 |= ENC + ADC10SC;    // Sampling and conversion start
}

```

Code for Data Transmitting

```

/*****
//
// Description: Data Transmitting
//
//      MSP430F1232
//      -----
//      /\ |           XIN|-----\
//      | |           | Crystal
//      |--RST      XOUT|-----^
//      |           |
//      |           P1.0|--> RF Transmitter
// sensor-->|ADC      |
//      -----
//
// David Johnson
// University of Florida
// August 2005
/*****

#include <msp430x12x2.h>

void main(void)
{
    WDTCTL = WDTPW + WDTHOLD;          // Stop WDT
    P3DIR |= 0x10;                     // Set P1.0 to output direction
    P3OUT = 0x00;                      // Set the output to 0x0
    ADC10CTL0 = ADC10SHT_2 + ADC10ON + ADC10IE;
    CCTL0 = CCIE;                      // CCR0 interrupt enabled
    CCR0 = 5000;                       // Delay for Sampling
    TACTL = TASSEL_1 + MC_1;           // ACLK, upmode

    _EINT();                           // Enable interrupts.
    ADC10AE |= 0x01;                   // P2.0 ADC option select
    LPM3;

}

// ADC10 interrupt service routine
#pragma vector=ADC10_VECTOR
__interrupt void ADC10_ISR (void)
{
    static int output_already;         // Variable to determine if Transmitted to Output
    if (ADC10MEM < 0x1FF)
    {
        P1OUT = 0x00;                 // Set output LOW
    }
}

```

```

// Delay data from being transmitted
int transmit_dly;
for (transmit_dly = 2000; transmit_dly>0; transmit_dly--);
int d_out = 0; // Loop variable for number of data bits
int temp = ADC10MEM;

while (d_out<10)
{
    P3OUT = (temp & 0x1) << 4;
    int i;
    for (i = 100; i>0; i--); // Wait with output set to bit value of sensor data
    temp = temp >> 1;
    d_out++;
}

P3OUT = 0x00; // Set output LOW
output_already = 0; // Reset variable
}

else if (output_already == 0)
{
    P1OUT = 0x00; // Set output LOW
    output_already = 1; // Set variable so transmission only occurs once
    // Encode and transmit ADC Sample
    int data_bit = 0; // Loop variable for number of data bits
    int temp2 = ADC10MEM;

    while (data_bit<10)
    {
        P1OUT = (temp2 & 0x1);
        int j;
        for (j = 100; j>0; j--); // Wait with output set to bit value of sensor data
        temp2 = temp2 >> 1;
        data_bit++;
    }

    P1OUT = 0x00; // Set output LOW
}

else // Occurs if Emergency Transmit sent already
{
    // Delay data from being transmitted
    int delay2;
    for (delay2 = 2000; delay2>0; delay2--);
    int d_out2 = 0; // Loop variable for number of data bits
    int temp2 = ADC10MEM;

```

```
while (d_out2<10)
{
    P3OUT = (temp2 & 0x1) << 4;
    int k;
    for (k = 100; k>0; k--);           // Wait with output set to bit value of sensor data
    temp2 = temp2 >> 1;
    d_out2++;
}

P3OUT = 0x00;           // Set output LOW
output_already = 1;    // Reset variable
}

}

// Timer A0 interrupt service routine
#pragma vector=TIMERA0_VECTOR
__interrupt void Timer_A (void)
{
    ADC10CTL0 |= ENC + ADC10SC;      // Sampling and conversion start
}
```

LIST OF REFERENCES

1. A. Siemens, "Facts about Solar Energy," <http://www.siemenssolar.com/facts.html>, Pacific Paradise, Australia, 2003, last accessed March 2006.
2. A. E. Messer, "Prototype Under-Skin Glucose Sensor," Medical News Today, <http://www.medicalnewstoday.com/medicalnews.php?newsid=31294>, Sept. 28, 2005, last accessed March 2006.
3. S. Roundy, P.K. Wright, and J.M. Rabaey, *Energy Scavenging for Wireless Sensor Networks with Special Focus on Vibrations*, Ch. 1, 22-23, Kluwer Academic Publishers, Norwell, Massachusetts, 2004.
4. Cap-XX, "GW1 Series – Double Layer Supercapacitor," Product Data Sheet, Cap-XX, Myrtle Beach, SC, 2006.
5. Freescale Semiconductor, "High Accuracy Digital Tire Pressure Gauge," AN1953 Product Application Note, Freescale Semiconductor, Austin, TX, 2006.
6. C. Murray, "Embedded Developers Do Some Sole Searching," Embedded.com, June 14, 2004.
7. Crossbow Technology, Inc., Product Information on MICA Mote, http://www.xbow.com/Products/Product_pdf_files/Wireless_pdf/MICA.pdf, Crossbow Technology, Inc., San Jose, CA, 2006, last accessed March 2006.
8. K. Pister, "Smart Dust: Autonomous Sensing and Communication in a Cubic Millimeter," <http://robotics.eecs.berkeley.edu/~pister/SmartDust/>, Berkeley, CA, 2001, last accessed March 2006.
9. MicroStrain, "EmbedSense Wireless Sensor," <http://www.microstrain.com/embed-sense.aspx>, MicroStrain, Williston, VT, 2005, last accessed March 2006.
10. Microstrain, "StrainLink," <http://www.microstrain.com/strain-link.aspx>, MicroStrain, Williston, VT, 2005, last accessed March 2006.
11. Coronis Systems, Homepage of Coronis Systems, <http://www.coronis-systems.com/>, Coronis Systems, Cambridge, MA, 2006, last accessed March 2006.

12. Dust Networks, Homepage of Dust Networks, <http://www.dustnetworks.com/flash-index.shtml>, Dust Networks, Hayward, CA, 2006, last accessed March 2006.
13. Crossbow Technology, Inc., “Wireless Sensor Networks,” http://www.xbow.com/Products/Wireless_Sensor_Networks.htm, Crossbow Technology, Inc., San Jose, CA, 2005, last accessed March 2006.
14. Cirronet Inc., Homepage of Cirronet Inc., <http://www.cirronet.com/>, Cirronet Inc., Duluth, GA, 2005, last accessed March 2006.
15. Intel Corporation, “Sensor Nets / RFID,” http://www.intel.com/research/exploratory/wireless_sensors.htm, Intel Corporation, Santa Clara, CA, 2006, last accessed March 2006.
16. W. Ye, J. Heidenmann, and D. Estrin, “An Energy-Efficient MAC Protocol for Wireless Sensor Networks,” Proceedings of 21st International Annual Joint Conference of the IEEE Computer and Communications Societies (Infocom 2002), volume 3, pages 3-12, June 2002.
17. IEEE, IEEE 802.15.4 Standard, <http://standards.ieee.org/getieee802/download/802.15.4-2003.pdf>, IEEE, Piscataway, NJ, 2006, last accessed March 2006.
18. ZigBee™ Alliance, Homepage of ZigBee™ Alliance, <http://www.zigbee.org/en/index.asp>, Global Inventors, Inc., San Ramon, CA, 2006, last accessed March 2006.
19. A. Rodzevski, J. Forsberg, and I. Kruzela, “Wireless Sensor Network with Bluetooth,” Proceedings of Smart Object Conference, Grenoble, France, May 2003.
20. J. M. Rabaey, M. J. A., J. L. da Silva Jr., D. Patel, and S. Roundy, “PicoRadio Supports Ad Hoc Ultra-Low Power Wireless Networking,” Computer Magazine, Vol. 33, No.7, pages 42-48, July 2000.
21. A. Dunkels, T. Voigt, and J. Alonso, “Connecting Wireless Sensor Networks with the Internet,” ERCIM News, No. 57, pages 61-62, April 2004.
22. A. Mason, N. Yazdi, K. Najafi, K. D. Wise, “A Low-Power Wireless Microinstrumentation System for Environmental Monitoring,” The 8th International Conference on Solid-State Sensors and Actuators, and Eurosensors IX, volume 19-A3, pages 107-110, June 1995.

23. M. Ismail, "A Novel Ultra Low Power CMOS Radio for Wireless Sensor Nodes (WiSeNode)," http://wireless.kth.se/menu/research/research_pdf/Wireless@KTH_SensorNodes_final_Sept2005.pdf, Wireless@KTH, Kista, Sweden, 2005, last accessed March 2006.
24. S. Roundy, P.K. Wright, and J.M. Rabaey, *Energy Scavenging for Wireless Sensor Networks with Special Focus on Vibrations*, Kluwer Academic Publishers, Norwell, Massachusetts, 2004.
25. S. Roundy, B. P. Otis, Y.-H. Chee, J. M. Rabaey, P. Wright, "A 1.9GHz RF Transmit Beacon using Environmentally Scavenged Energy," ISPLED 2003, August 25-27, 2003, Seoul, Korea.
26. E. S. Leland, E. M. Lai, P. K. Wright, "A Self-Powered Wireless Sensor for Indoor Environmental Monitoring," 2004 Wireless Networking Symposium, University of Texas, Austin, October 20-22, 2004.
27. Texas Instruments, "MSP430x11x2, MSP439x12x2 Mixed Signal Microcontroller," Product Datasheet, Texas Instruments, Dallas, TX, 2004.
28. Ming Microsystem, Inc., "TX-99 V3.0 RF Transmitter Board," Product Datasheet, Reynolds Electronics, Canon City, CO, 2005.
29. Radio Innovation, "How Far Will My Radio Transmit?" http://www.radioinnovation.com/Howto/how_far.htm, Radio Innovation, 2005, last accessed March 2006.
30. D. L. Ash, "A Comparison between OOK/ASK and FSK Modulation Techniques for Radio Links," <http://www.rfm.com/products/apnotes/ookvsfsk.pdf>, RF Monolithics, Inc., Dallas, Texas, 2006, last accessed March 2006.
31. Protel International Pty. Ltd., *Protel v. 4.0.16 User's Guide*, Altium Limited, San Diego, CA, 1998.
32. LPKF Laser & Electronics AG, *LPKF ProtoMat 91s/HS Manual*, Part #106 049, LPKF Laser & Electronics AG, Wilsonville, OR, May 1998.
33. IXYS Corporation, "IXOLARTM High Efficiency Solar Cells," XOD17 Product Datasheet, IXYS Corporation, Santa Clara, CA, 2005.
34. S. Xu, K. Ngo, T. Nishida, G. B. Chung, A. Sharma, "Converter and Controller for Micro-Power Energy Harvesting," 20th Annual IEEE Applied Power Electronics Conference and Exposition, Vol. 1, pp. 226-230, March 2005.
35. S. Meninger, J. O. Mur-Miranda, R. Amirtharajah, A. P. Chandrakadan, and J. H. Lang, "Vibration-to-Electric Energy Conversion," IEEE Trans. on VLSI systems, vol. 9, pp. 64-76, February 2001.

36. Piezo Systems, Inc., "Standard Double Quick-Mount Bending Actuators," Product Information Page, <http://www.piezo.com/prodbm8dqm.html>, Piezo Systems, Inc., Cambridge, MA, 2006, last accessed March 2006.
37. Piezo Systems, Inc., "PSI-SA4E Single Layer Disks," Product Information Page, <http://www.piezo.com/prodsheet3disk5A.html>, Piezo Systems, Inc., Cambridge, MA, 2006, last accessed March 2006.
38. L. C. Tien, P. W. Sadik, D. P. Notron, L. F. Voss, S. J. Pearton, H. T. Wang, B. S. Kang, F. Ren, J. Jun, and J. Lin, "Hydrogen-Selective Sensing at Room Temperature with ZnO Nanorods," *Appl. Phys. Lett.* 87, 222106(2005).

BIOGRAPHICAL SKETCH

David E. Johnson was born on July 14, 1977, in Toms River, New Jersey. He moved to Jacksonville, Florida, where he graduated from Samuel Wolfson High School in 1995. He earned a B.S. in electrical engineering and a B.S. in computer engineering from the University of Florida, in December 2000. During his undergraduate time at the University of Florida he maintained research positions working for two different research groups: Interdisciplinary Center for Aeronomy and Other Atmospheric Sciences (ICAAS) and Interdisciplinary Microsystems Group (IMG). Upon finishing his bachelor's degrees, he took a position working for Cisco Systems as a Hardware Engineer. While working for Cisco Systems he continued part time at the University of Florida in pursuit of a M.S. in electrical engineering. He intends to graduate from the University of Florida in May 2006 with a M.S. in electrical engineering. Upon graduation he plans to continue working for Cisco Systems.